CORA Cork Open Research Archive
Cartlann Taighde Oscailte Chorcaí

Title	Inertial sensors-based lower-limb rehabilitation assessment: A comprehensive evaluation of gait, kinematic and statistical metrics
Authors	Tedesco, Salvatore;Urru, Andrea;Peckitt, James;O'Flynn, Brendan
Publication date	2017
Original Citation	Tedesco, S., Urru, A., Peckitt, J. and O'Flynn, B. (2017) 'Inertial Sensors-based Lower-Limb Rehabilitation Assessment: A Comprehensive Evaluation of Gait, Kinematic and Statistical Metrics', International Journal on Advances in Life Sciences, 9 (1 & 2), pp. 33-49.
Type of publication	Article (peer-reviewed)
Link to publisher's version	http://www.iariajournals.org/life_sciences/tocv9n12.html
Rights	2017, © Copyright by authors, Published under agreement with IARIA - www.iaria.org
Download date	2026-11-06 21:52:47
Item downloaded from	https://hdl.handle.net/10468/5624

UCC
University College Cork, Ireland
Coláiste na hOllscoile Corcaigh

Inertial Sensors-based Lower-Limb Rehabilitation Assessment: A Comprehensive Evaluation of Gait, Kinematic and Statistical Metrics

Salvatore Tedesco[1], Andrea Urru[1], James Peckitt[2], Brendan O'Flynn[1]
[1]WSN Group, Micro & Nano Systems - Tyndall National Institute
[2] Mardyke Arena Clinic
University College Cork
Cork, Ireland
e-mail: salvatore.tedesco@tyndall.ie

Abstract— **Analysis of biomechanics is frequently used in both clinical and sporting practice in order to assess human motion and their performance of defined tasks. Whilst camera-based motion capture systems have long been regarded as the 'Gold-standard' for quantitative movement-based analysis, their application is not without limitations as regards potential sources of variability in measurements, high cost, and practicality of use for larger patient/subject groups. Another more practical approach, which presents itself as a viable solution to biomechanical motion capture and monitoring in sporting and patient groups, is through the use of small-size low-cost wearable Micro-ElectroMechanical Systems (MEMs)-based inertial sensors. The clinical aim of the present work is to evaluate rehabilitation progress following knee injuries, identifying a number of metrics measured via a wireless inertial sensing system. Several metrics in the time-domain have been considered to be reliable for measuring and quantifying patient progress across multiple exercises in different activities. This system was developed at the Tyndall National Institute and is able to provide a complete and accurate biomechanics assessment without the constraints of a motion capture laboratory. The results show that inertial sensors can be used for a quantitative assessment of knee joint mobility, providing valuable information to clinical experts as regards the trend of patient progress over the course of rehabilitation.**

Keywords- Inertial Sensors; Wearable Microsystems; Signal Processing; Data Analytics; Lower-Limb Rehabilitation; Motor Performance.

I. INTRODUCTION

This paper is an extended presentation of [1], a study on the qualitative assessment of progress during rehabilitation via wearable inertial sensors, first published at Global Health 2016.

Biomechanics is the science related to the study of the internal and external forces acting on the human body and the effects produced by them [2]. In particular, one aspect of biomechanics analysis is the study of human locomotion and of the forces causing movement and human kinetics.

This analysis is frequently used in both clinical and sporting practice by clinicians and can play a crucial role in athletes' performance enhancement, injury prevention, and effective rehabilitation. More specifically, in the latter case, it is essential to track patient progress, and consequently to tailor patients-oriented rehabilitation programs, through the accurate assessment of human motion during the performance of clinically defined tasks.

A common example of the technology regarded as being the 'Gold-standard' of quantitative movement analysis is shown by camera-based motion analysis systems (such as the ones provided by Vicon [3], Optitrack [4], or Codamotion [5]) which, during formal gait analysis by rehabilitation professionals, can help to ascertain measurements of Temporal (Time) and Spatial (Distance) characteristics associated with gait parameters. This enables clinicians to identify gait deviations in paediatric and amputee populations, in screening elderly people at risk of falling, to objectively monitor a patient's progress, and to help determine the efficacy of surgical and therapy interventions [6-9].

While camera-based motion capture systems achieve very high performance, their application is not without limitations as regards potential sources of variability in measurements, relatively high costs of instrumentation including access to specialist motion labs, as well as practicality of application for larger patient/subject groups, as discussed by Chau et al. in [10]. Similar drawbacks have been demonstrated for other accurate, clinical grade, gold-standard measurement systems, such as marker less video [11], instrumented treadmills [12], walkway contact mats [13], or force platforms [14].

From a clinical perspective, observational forms of clinical gait analysis frequently forms the corner stone of patient knee joint assessment, and is typically used in parallel with manual clinical assessment techniques. These include stress-testing evaluation of joint laxity, range of movement (ROM), and manual and/or isokinetic strength assessment, as well as contextual subjective patient questionnaires, such as Knee Injury and Osteoarthritis Outcome Score (KOOS), Oxford Knee Score (OKS), Tegner Lysholm Knee Scoring Scale, International Knee Documentation Committee (IKDC), and Western Ontario & McMaster Universities Osteoarthritis Index (WOMAC) [15][16], which employ a high degree of patient involvement.

However, the use of observational gait analysis (non-empirical assessments), even when utilised by experienced clinicians, may not be adequate or sensitive enough to detect subtle clinical pathological changes in movement following knee surgery [8] [9].

2017, © Copyright by authors, Published under agreement with IARIA - www.iaria.org

An alternative approach, which has been explored as a more practical and viable solution to biomechanical motion capture and monitoring in sporting and patient groups, involves the use of small-size low-cost wearable inertial sensors [17].

There has been a wide variety of work presented in literature on inertial sensors applied to biomechanics. These have been typically adopted for monitoring the lower-limbs during rehabilitation or tele-rehabilitation and used to objectively assess the performance of impaired subjects throughout the process, in particular following knee injuries. However, most of those investigations were focused on a one-time assessment rather than a longitudinal evaluation over several weeks looking at change in gait over longer periods.

The aim of the present work is to evaluate motor performance during lower-limb rehabilitation targeting activities normally assigned by clinicians for at-home rehabilitation. The work also addresses the assessment of the performance of body-worn kinematic sensors in a rehabilitative context, given their well-known potential in accurately extracting parameters that inform qualitatively and quantitatively movement parameters.

Informed by clinical partners involved in the development and validation of the system, the study investigates and derives a number of features and metrics, related to gait and kinematic characteristics and statistical analysis. These data sets will be analysed to establish which of them are the most sensitive and helpful to determine changes in motor capacity over a longitudinal study of nine months. The data sets acquired will help develop, in future works, better models for objectively estimating the conditions and the motor performance of adults involved in lower-limb at-home rehabilitation following knee injuries.

The derived outcome of this model will be analyzed by clinicians and sport scientists to gain a comprehensive picture of patients' condition and provide more targeted medical feedback.

The analysis is carried out by using a wearable inertial sensing system developed at the Tyndall National Institute, consisting of two sensors per limb, which is able to provide a complete biomechanics assessment for a series of scripted activities, based on best clinical practice.

The present work is organized as follows. Relevant recent works are discussed in Section II while the description of the hardware and of the test protocol used during the data collection are described in Section III. The methodology behind the feature selection is illustrated in Section IV. The obtained results are shown in Section V and exhaustively analyzed and discussed. Finally, conclusions are drawn in the last section.

II. Related Works

Inertial sensors are generally used in devices to measure velocity, orientation, and gravitational force, and are used in a great number of applications. These include industry quality control, robotics, navigation systems, sports, augmented reality systems, and so on [18-21]. Biomechanics, in particular, has achieved significant progress from the adoption of this technology [22].

More specifically, with regards to gait analysis, accelerometers and gyroscopes have been used worn on the lower-limbs to obtain gait parameters [23-26], which can be derived by the integration of linear acceleration or angular velocity, after the correct identification of the beginning and the end of each gait cycle. Interesting innovations have been proposed in [27] by L. Atallah et al. in the development of an ear-worn sensor for gait monitoring, or by S. Kobashi et al. [28] who included magnetic sensors in combination with inertial sensing to estimate knee joint angle in three dimensions.

This technology has not only been taken into account for healthy subjects. Such systems have also been used for the detection of pathologic conditions, discriminating clinical indications between symptomatic and asymptomatic subjects in a number of diseases. Conditions which have been investigated in this way include cerebral palsy [29], hemiplegia [30-31], Parkinson's [32], dementia [33], old age [34], and Anterior Cruciate Ligament (ACL) injury [35].

In recent years, researchers have increasingly been investigating the use of inertial sensors in gait rehabilitation. Most of the studies in this area focused on the implementation of a lower-limb monitoring system for remote rehabilitation or tele-rehabilitation [36-38], or in the performance assessment of specific rehabilitation exercises [39-46]. In the latter case, machine learning techniques are adopted to discriminate between the correct and incorrect execution of recommended exercises. The most advanced techniques can also highlight if multiple incorrect postures are present while performing the test. Typically, a number of body-worn sensors are used for the classification. However, there is a significant body of research in the investigation of the efficacy of the adoption of only one sensor [47-50]. This can be obtained also through the adoption of specific biomechanical models related to particular exercises.

Immersive virtual reality, computer games, or visualization tools are recently being developed in order to enhance patients' adherence to the rehabilitation program and enhance motivation [51-53]. The accuracy and reliability of those inertial sensors and biofeedback-based rehabilitation systems have been shown in [54-55].

To date, however, few studies considered the quantitative assessment of patients' lower-limb performance via body-worn sensors during the complete rehabilitation process. This task is particularly challenging as it consists of isolating the gradual changes in movements due to recovery and improvement despite the presence of a multitude of sources of variability. The temporal and spatial sources of intra- and inter-variability (e.g., dissimilarities in repetitions of an exercise when performed by one subject, and dissimilarities between different subjects, respectively) are already evident

2017, © Copyright by authors, Published under agreement with IARIA - www.iaria.org

in healthy subjects, given the different characteristics of gender, age, height, and weight, etc…, and are even more significant in patients following rehabilitation, due to different levels of pain, fatigue, and possible compensations.

For instance, Lin et al. [56] estimated the joint angles with a novel extended Kalman filter on 14 exercises performed by a cohort of elderly patients monitored from the first day of admission until discharge, with the average patient's treatment lasting 5.7 days.

Similarly, Field et al. [57] investigated the gradual changes of motion with new proposed metrics, by monitoring the symmetry between the left and right sides of the body for 14 subjects over repeated rehabilitation exercises in a period of 12 weeks. However, despite the completeness of the method, the study required the patient to wear a motion capture suit consisting of 17 sensors, which is cumbersome and not feasible for at-home rehabilitation.

Finally, in [58], a novel machine learning technique has been proposed that estimates the continuous measurement of patient improvement which is capable of handling a variety of rehabilitative exercises. The approach was tested by adopting two wearables sensors on thigh and shank on clinical data collected on 18 elderly patients involved in rehabilitation following hip and knee replacements for a range of 4-12 days.

However, the main limitations of those studies are related to the short period for data collection which explores only the initial part of the rehabilitative process without considering the long-term effects or the pre-surgery conditions. Another limitation is the need of a large and specific initial dataset on which the machine learning method has to be trained. Finally, the lack of definition of the variation of the selected features throughout the analysis period and their impact on the final outcome is a constraint in using this approach.

The present study, as an extended version of [1], will analyze the data collected from a patient in pre/post-surgery conditions for an overall period over nine months, with the twofold aim of:

1. investigating, through body-worn inertial sensing, the effects of rehabilitation over different periods, also in the long-term, monitoring patient's progress,
2. understanding which parameters, taken from a wide range of features described in literature, and informed by clinical inputs, can be the most beneficial and sensitive for clinicians when monitoring patients in the course of lower-limb rehabilitation.

III. Hardware and Protocol for Data Collection

The biomechanical monitoring system consists of two Tyndall Wireless Inertial Measurement Units (WIMUs) [59] per leg, each one with 3D accelerometer and gyroscope (@ 250 Hz) and Bluetooth Low-Energy for wireless communication (Figure 1). WIMUs have been attached to the anterior tibia, 10 cm below the tibial tuberosity, and to the lateral thigh, 15 cm above the tibial tuberosity using surgical adhesive tape.

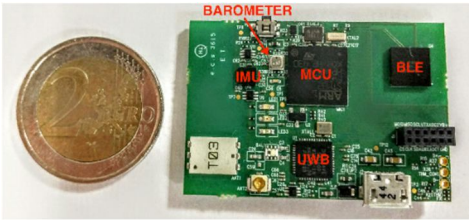


Figure 1. Tyndall Wireless Inertial Measurement Unit (WIMU)

The rehabilitation exercises (or scenarios) considered are walking, half squat, hamstring curl, and flexion/extension – defined by physiotherapists as good indicators of rehabilitation progress. These are described as follows:

- In the walking scenario, the subject walks on a treadmill, which is operated at defined speeds (3-4-6 km/h) for approximately one minute per test.
- In the half squat scenario, the subject stands with the feet shoulder's distance apart and arms crossed on the chest. Keeping the chest lifted, the hips are lowered about 10 inches, planting the weight in the heels. The body is then brought back up to standing by pushing through the heels.
- In the hamstring curl scenario, the subject stands and bends the knee raising the heel toward the ceiling as far as possible without pain, relaxing the leg after each repetition. This is repeated on both legs.
- In the flexion/extension scenario, the subject lies supine on the floor and bends the knee raising it toward the chest as far as possible without pain, relaxing the leg after each repetition. This is repeated on both legs.

The system has been tested with an impaired subject. The impaired subject is a female athlete, age: 44, height: 161 cm, and weight: 52 kg, with good general health status, with a history of knee injuries and surgery (reconstructed anterior cruciate ligament in the left leg following a sporting injury). The tests were carried out during the course of the rehabilitation program, e.g., starting 1 month before surgery and finishing 7 months after surgery. Overall, the subject has been evaluated through three periods: once in pre-surgery conditions (e.g., 1 month before surgery), then 6 times in a range of 20 weeks starting one month after surgery (namely short-term post-surgery), and finally once 3 months after the last data capture (e.g., during long-term post-surgery period).

A number of repetitions has been collected for each scenario, so as to provide an accurate picture of the overall conditions, and each scenario was evaluated during almost every data capture. The hamstring curl scenario as well as the walking test at 3 and 4 km/h was performed at every session.

2017, © Copyright by authors, Published under agreement with IARIA - www.iaria.org

Similarly, the flexion/extension test was always recorded except in the pre-surgery session due to subject's impairment of movement. For the same reason, half squat and walking at 6 km/h were not recorded in the first 2 sessions of the short-term post-surgery period.

IV. FEATURES SELECTION

The metrics taken into account for the patient's assessment are divided into three main categories: statistical metrics, gait characteristics, and time-domain kinematic measurements.

i. Statistical Features

This category takes into account various well-known statistical features extrapolated from the time-domain. Those variables are applied on every segmented walking stride/exercise repetition for both legs performed during the sessions. The selected features are described below:

- Mean, standard deviation, variance, skew, kurtosis, root mean square, signal magnitude area, energy (given by the integration over the repetition of the squared absolute signal) of the acceleration and angular velocity magnitudes;
- Mean, minimum, maximum, median, standard deviation, coefficient of variation (CV), peak-to-peak (PP) amplitude, and root mean square of the x-, y-, and z-axis of the acceleration and angular rate signals;
- Autocorrelation on the x-, y-, and z-axis of the acceleration and angular rate signals measured taking into account all the repetitions/strides in a session as a whole and not separately.

All those features are calculated for each of the 4 sensors used for data collection.

ii. Gait Characteristics

Well-known gait measures [1] are calculated from the data recorded by the inertial sensors attached on the shanks as follows:

- Gait cycle time (GCT), which is the time-interval between two consecutive toe-offs of the same leg;
- Stance phase, defined as the weight-bearing phase of the GCT in which the body is supported, and is expressed by the difference between a heel-strike and the following toe-off of the same leg;
- Relative stance phase, the ratio between stance phase and GCT;
- Swing phase, which is the non-weight bearing phase of GCT, and is expressed by the difference between a heel-strike and the previous toe-off of the same leg;
- Relative swing phase, the ratio between the swing phase and the GCT;
- Double support, the time-interval when both feet are in ground contact;
- Stride length, indicated as the distance between two successive placements of the same foot, computed as the total trajectory on the sagittal plane made by the sensor attached to the shank. The approach is based on a double integration of inertial data collected in a stride. The integration process is reset at the end of each stride;
- Stride speed, computed by the ratio between stride length and GCT;
- Clearance, defined as the maximum height reached by the sensor during the swing phase and obtained by the vertical displacement calculated to establish the stride length during the swing phase.

For each variable, also the related CV has been extrapolated, and consequently, also the associated symmetry, defined for each specific parameter as

$$Symmetry_{parameter} = \frac{|CV_{parameter_left} - CV_{parameter_right}|}{\mu(stride_speed)} \quad (1)$$

where $\mu(\text{stride_speed})$ is the average of the measured stride speed for that specific session.

Moreover, the Balance Index (B.I.), as shown in [31], expressed as the absolute ratio between the difference of the left and right leg's values of a specific gait parameter and their sum, was obtained for all the variables.

This information is obtained for both legs for the walking scenario only.

iii. Kinematic Variables

Finally, the third category is related to kinematic metrics, occasionally adopted for gait analysis, but that can provide useful information on the movement analysis, and have been proposed in recent works in literature. Those metrics are as follows:

- Knee Range of Motion (ROM), defined as the peak-to-peak amplitude of the knee joint angle during a repetition;
- Regularity [60], e.g., the ratio between the unbiased autocorrelation coefficient at the first dominant period and the coefficient at the second dominant period, both measured taking into account all the repetitions within the same analyzed scenario;
- Range of Angular Velocity (RANG) [61-62]: the difference between the minimum and the maximal value of the angular velocity magnitude within each repetition;
- Jerk-based smoothness measures, where the jerk is the rate of change of the acceleration in a repetition. Several jerk-based metrics have been proposed, including integrated squared jerk (ISJ), mean squared jerk (MSJ),

2017, © Copyright by authors, Published under agreement with IARIA - www.iaria.org

cumulative square jerk (CSJ), root mean square jerk (RMSJ), mean square jerk normalized by peak speed (N_MSJ), integrated absolute jerk (IAJ), mean absolute jerk normalized by peak speed (N_MAJ), and dimensionless square jerk, whose mathematical definitions are shown in [63];

- Vertical acceleration [64], defined as the maximum value over a repetition of the difference between the acceleration magnitude (filtered with a 2nd order Butterworth low-pass filter with cut-off frequency 3 Hz) and the gravitational force;
- Vertical velocity [64], defined as the integration over a repetition of the difference between the acceleration magnitude (filtered with a 2nd order Butterworth low-pass filter with cut-off frequency 3 Hz) and the gravitational force;
- Fluency [64], e.g., the integration over a repetition of the absolute difference between the raw and the filtered x, y, and z-axis acceleration signals. Again the filter used is a 2nd order Butterworth low-pass filter with cut-off frequency 3 Hz;
- Stability [65], defined as the dynamic time warping of the x-, y-, and z-axis of the acceleration and angular rate signals measured at two consecutive repetitions/strides, then averaged based on all the repetitions present in a test session;
- Kinetic Value (KV) [66], defined as the squared integral of the magnitude of the acceleration signal over a repetition, multiplied by *m/2*, where *m* is the subject's body weight.

All those features in this class are calculated for each of the 4 sensors used for data collection.

The data analysis is implemented off-line over the data collected using a commercial software package (MATLAB R2015a, The MathWorks Inc., Natick, MA, 2015) [67]. Each repetition/stride was visually segmented.

V. Results and Discussion

In each session, each scenario was divided in two separate tests (both logged for 60 sec), and in each of the two tests a series of repetitions have been carried out by the subject. The overall number of repetitions recorded for all the sessions was: 184 hamstring curls (92 left and 92 right), 134 flexion/extensions (67 left and 67 right), 66 half squats, 478 strides for both legs when walking at 3 km/h, and similarly 544 strides when walking at 4 km/h, and 512 strides when walking at 6 km/h. For each test, the features described in Section IV were extrapolated and compared among the different sessions, in order to provide a clear understanding of which metrics can be more valuable during rehabilitation. The results are summarized in different tables (collected in the Appendix, which is available as a PDF file at the following link: https://www.tyndall.ie/contentfiles/Tables_IARIA.pdf) where each table consists of 9 columns given by all the sessions in which the test were carried out. Each session is divided in three sub-columns: one for indicating the results for the left leg, one for the right leg, and the last one for the mean difference (expressed in percentage) between left/right values (considering the right leg values as references), the Pearson's r coefficient and the p-value between the left/right leg results, calculated when appropriate. The sub-columns related to left and right results are merged in case of gait metrics which in their calculation takes into account aspects from both legs. Due to the fact that the subject could not perform all the scenarios during each session, not all the columns in the tables are filled. Moreover, owing to malfunctioning issues during data recording, results from the right leg in the hamstring curl scenario on the first session are not available.

Given the number of tables extrapolated from the data, only a small subset of those tables are included in this paper for clarification, while full details are shown in the Appendix.

The mean difference, in particular, is an important estimator of the dissimilarities between the two legs which, in an ideal case, should be close to zero in any case for a healthy unimpaired subject. Given its definition, negative values of the mean difference indicate that results for the right leg are larger compared to the left one, and *vice versa* for positive values.

Finally, in order to have the same reference system for both WIMUs worn on the same leg, the method proposed by Seel et al. [68] has been adopted to virtually rotate around an axis the raw inertial data recorded on the shank. As a result, for all the WIMUs involved, the x-axis represents the medio-lateral axis, the y-axis is the anteroposterior one, while the z-axis is the vertical axis. Thus, the plane y-z represents the sagittal plane.

Results from data analysis, divided in three categories, are described below.

i. Gait Metrics

The analysis performed on the gait characteristics is summarized in Tables I-II-III available in the Appendix and in this paper, which represents the walking test at 3, 4, and 6 km/h, respectively. All the gait features are indicated in those tables, with B.I. and symmetry calculated for each metrics and shown together in the same row.

Considering the gait results at 3 km/h, there are several metrics which may be beneficial for showing the patient's progress during rehabilitation. As an example, even though the p-value related to the GCT in all sessions is above 0.05 (e.g., there is no statistical difference between the two legs), the calculated mean difference between left/right for this parameter has a clear convergence to zero during the monitoring phase, and the same trends are evident also for the mean difference of the CV, B.I., and symmetry associated to GCT. Similar considerations can be observed in the results

2017, © Copyright by authors, Published under agreement with IARIA - www.iaria.org

provided by the CV obtained for the stance phase, swing phase, and double support. In particular, the mean difference associated to the CV of the stance phase shows a convergence after the second session, as it is evident a clear increase of the mean difference between the first two sessions (the pre-surgery session, and the first test after surgery), due to the early stage of the recovery process post-surgery.

Again, even though the p-values for the stride length is constantly below 0.05 in the different sessions (e.g., there is always a significant difference between the two legs), the Pearson's coefficient continuously increases, while the mean difference tends to zero. The mean difference of the CV and the B.I. of the stride length shows a comparable convergence as well, also for what concerns the dissimilarities between the pre-surgery session and the first post-surgery one. Similar considerations may be drawn for the stride speed, also explained by the uniformity of the results given by the GCT.

The gait scenario at 4 km/h shows similar trends for the GCT-related parameters, and the mean difference of the CV related to the stance phase and double support, with an evident convergence towards zero and a strong disparity in the first two sessions. However, no particular correlation is clear for the stride length values. On the other hand, clearance may highlight some significant information. P-values are always lower than the statistical threshold (0.05), except that in the last session recorded seven months after surgery, and its mean difference and the B.I. measure show a clear convergence toward zero during the rehabilitation assessment, indicating, thus, a certain gained equivalence between the two legs.

Finally, gait results at 6 km/h show significant trends only for what concerns the mean difference of the CV of the double support and clearance-related parameters.

In summary, it is evident how, at slow speed, temporal parameters (especially indicated through their CV) and the stride length values should be considered for assessing differences between left and right legs during rehabilitation, whereas, increasing the speed, clearance seems to gain higher priority than time-related parameters. Only the mean difference of the CV of the double support shows a similar trend at all the tested speeds. Some of the discussed results are illustrated in Figures 2-4. The markers in the figures indicate the mean value obtained for a specific session, while the green line is a reference for zero.

ii. Statistical Features

The statistical features described in Section IV has been calculated for each repetition/stride for all the four WIMUs adopted and for both acceleration and angular rate signals. Results are summarized for all the scenarios in the tables in the Appendix and discussed below.

In the hamstring curl scenario, for example, the thigh is not significantly involved in the movement. Indeed, there are no specific variables showing improvements. Conversely, the shank is more informative. Standard deviation, variance, calculated on the acceleration magnitude, and standard deviation, CV, and peak-to-peak amplitude obtained from the z-axis acceleration all show clear convergences. Moreover, those trends are even more evident from metrics obtained by the angular rate collected on the shank. For instance, mean, standard deviation, variance, level of skew, signal magnitude area calculated from the magnitude signal, and minimum, maximum, standard deviation, and peak-to-peak amplitude on the three axis are all significant variables (Figure 5).

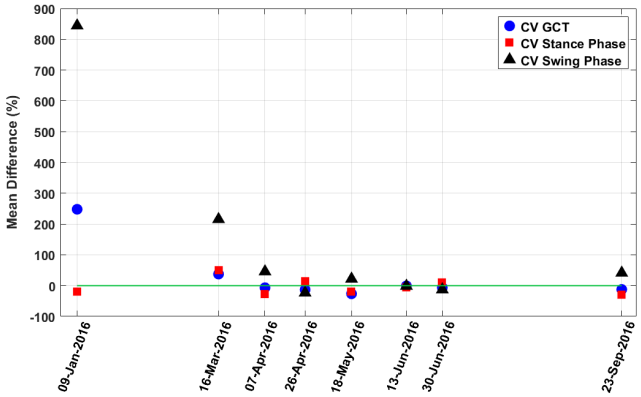


Figure 2. Mean difference for different gait parameters at 3 km/h showing the trends of progress during rehabilitation. CV GCT/stance phase/swing phase are shown

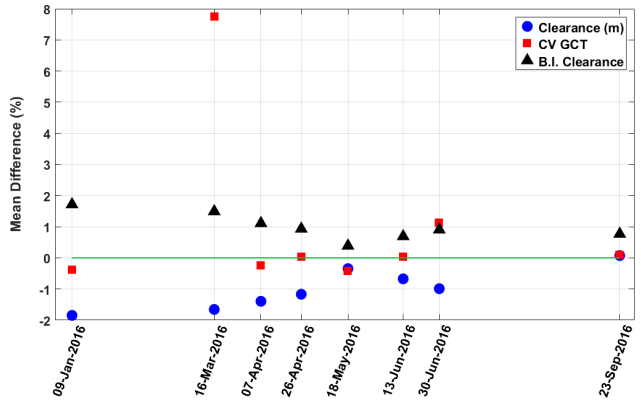


Figure 3. Mean difference and balance index for different gait parameters at 4 km/h showing the trends of progress during rehabilitation. Clearance CV GCT, and B.I. clearance are shown. Each variable is normalized according to its mean value for visualization purposes

In the flexion/extension scenario, the movement requires a higher involvement of the thigh compared to the curl which, thus, present several metrics useful for progress monitoring (Figure 6). Examples are the mean, standard deviation, variance, skewness, kurtosis, signal magnitude area, and energy obtained from the angular rate magnitude, minumum, standard deviation CV, and peak-to-peak amplitude from the acceleration vertical axis, and minimum, maximum, standard deviation, and peak-to-peak amplitude from the angular rate collected around the sagittal axis. There are also numerous metrics related to the shank, such as the mean, standard

2017, © Copyright by authors, Published under agreement with IARIA - www.iaria.org

deviation, variance, skewness, signal magnitude area, and energy obtained from the acceleration and angular rate magnitude, and a number of variables obtained from the single axis of the inertial sensors and associated to the sagittal plane. This higher number of metrics is due to the intrinsic movement as defined by the exercise which occurs almost completely on the sagittal plane and, thus, the information is highlighted around the rotation axis and not divided along the three axes. Indeed, this characteristic is not present in the remaining scenarios.

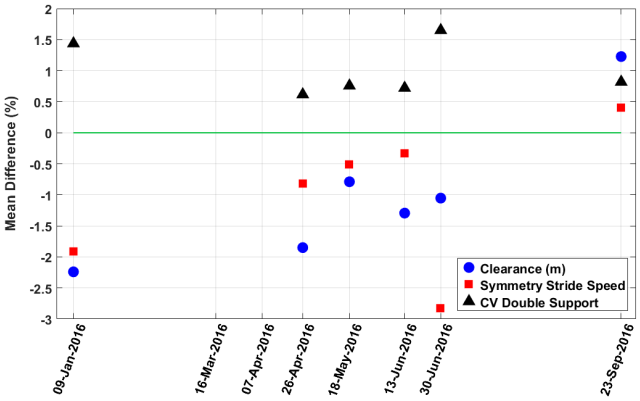


Figure 4. Mean difference and symmetry for different gait parameters at 6 km/h showing the trends of progress during rehabilitation. Clearance, symmetry stride speed, and CV double support are shown. Each variable is normalized according to its mean value for visualization purposes

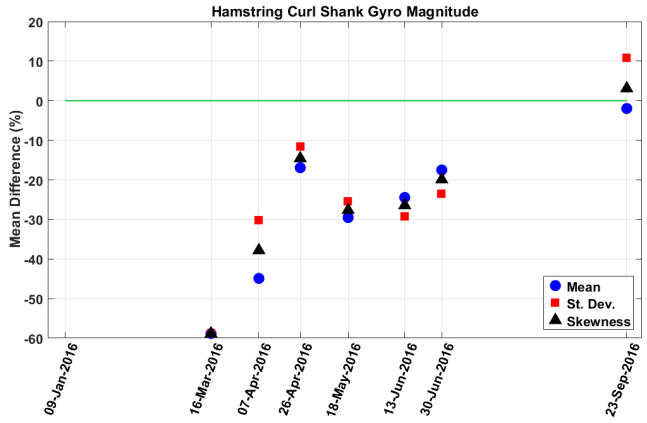


Figure 5. Mean difference for different statistical parameters in the curl scenario showing the trends of progress during rehabilitation. Mean/St. dev/skewness for the gyro shank magnitude are shown

In the half squat scenario only a few metrics are evident on separate axes. For example, the maximum and peak-to-peak value of the acceleration on the y-, z-axis measured on the thigh and shank, and the standard deviation, CV, and peak-to-peak amplitude measured along the sagittal axis on the angular rate of the lower-limbs illustrate a reasonable progress during the rehabilitation period, while the metrics (mean, level of skew, area, energy) calculated from the magnitude of the inertial data on the shank are more informative (Figure 7).

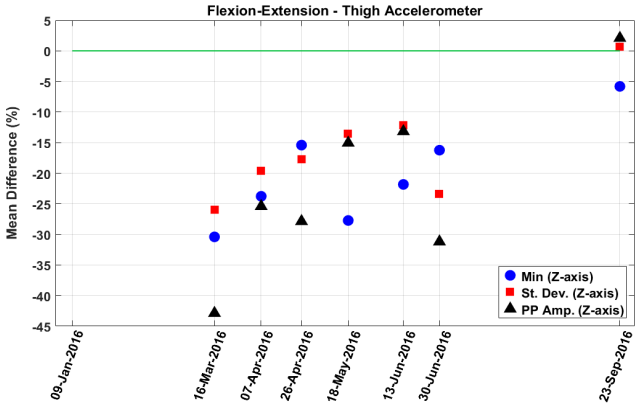


Figure 6. Mean difference for different statistical parameters in the flexion/extension scenario showing the trends of progress during rehabilitation. Minimum/st dev/PP amplitude for the acceleration thigh z-axis are shown

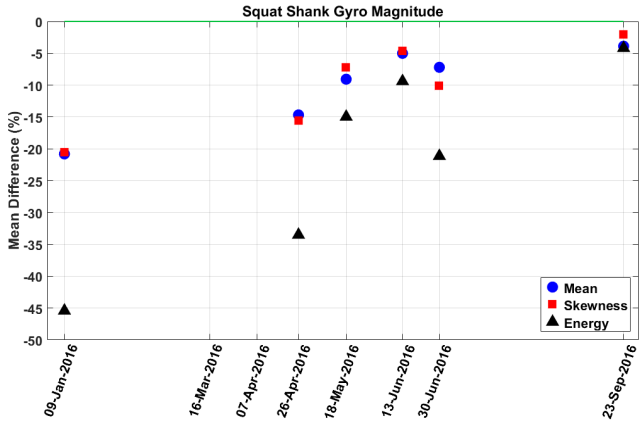


Figure 7. Mean difference for different statistical parameters in the half squat scenario showing the trends of progress during rehabilitation. Mean/skewness/energy for the gyro shank magnitude are shown

Similar considerations are evident on the gait test (Figures 8-10). The level of thigh movement, in this scenario, is not particularly informative, except for a reduced number of variables. Examples of these parameters are the root mean square calculated on the gyro magnitude and the standard deviation of the gyro around the vertical axis (when walking at 3 km/h), the CV of the acceleration/angular rate around the z-axis, and the maximum of the angular rate around the mediolateral axis (when walking at 4 km/h), and mean/peak-to-peak amplitude over the gyro x-axis, and the minimum of the gyro z-axis (when walking at 6 km/h). A higher number of helpful metrics is instead detected in the inertial data collected on the shank consistently for all the speeds. For instance, variables obtained from the acceleration magnitude can reliably show patient's progress over the rehabilitation course still highlighting the difference between left and right leg. Some parameters can be the mean, standard deviation, variance, level of skew, signal magnitude area, and energy when walking at slow speed, while increasing the speed may reduce the number of metrics to the standard deviation and

2017, © Copyright by authors, Published under agreement with IARIA - www.iaria.org

TABLE I. GAIT METRICS (3 KM/H)

GAIT 3KM/H	1st SESSION (09/01/2016)			2nd SESSION (16/03/16)			3rd SESSION (07/04/2016)			4th SESSION (26/04/16)		
Parameters	**R**	**L**	**Mean Diff. (%) / Paerson's r / p-value**	**R**	**L**	**Mean Diff. (%) / Paerson's r / p-value**	**R**	**L**	**Mean Diff. (%) / Paerson's r / p-value**	**R**	**L**	**Mean Diff. (%) / Paerson's r / p-value**
GCT (s)	1.386±0.030	1.346±0.102	-2.818/0.148/**0.045**	1.347±0.042	1.342±0.057	-0.397/0.356/0.671	1.387±0.032	1.379±0.030	-0.541/0.482/0.334	1.409±0.026	1.398±0.023	-0.755/0.457/0.090
CV_GCT (%)	2.177	7.574	247.880/-/-	3.107	4.27	37.414/-/-	2.309	2.152	-6.816/-/-	1.878	1.631	-13.155/-/-
B.I./Symmetry_GCT	0.022±0.039 / -3.895		-/-/-	0.015±0.015 / -0.863		-/-/-	0.008±0.009 / 0.113		-/-/-	0.007±0.007 / 0.175		-/-/-
Stance Phase (s)	0.886±0.020	0.864±0.020	-2.473/-0.042/**<0.001**	0.869±0.029	0.863±0.042	-0.707/0.101/0.500	0.896±0.026	0.871±0.018	-2.805/-0.057/**<0.001**	0.916±0.021	0.886±0.023	-3.232/0.211/**<0.001**
CV_Stance Phase (%)	2.945	2.34	-20.552/-/-	3.294	4.92	49.378/-/-	2.912	2.098	-27.965/-/-	2.287	2.609	14.116/-/-
B.I./Symmetry Stance Phase	0.019±0.013 / 3.887		-/-/-	0.024±0.014 / -0.485		-/-/-	0.019±0.013 / 0.039		-/-/-	0.018±0.014 / -0.700		-/-/-
Swing Phase (s)	0.500±0.011	0.483±0.103	-3.430/-0.089/0.356	0.478±0.016	0.479±0.051	0.165/0.339/0.933	0.491±0.019	0.509±0.028	3.589/0.167/**0.005**	0.493±0.013	0.512±0.010	3.842/0.016/**<0.001**
CV_Swing Phase (%)	2259	21.334	844.264/-/-	3.354	10.576	215.319/-/-	3.807	5.544	45.650/-/-	2.537	1.949	-23.182/-/-
B.I./Symmetry Swing Phase	0.063±0.142 / -20.762		-/-/-	0.044±0.026 / -8.383		-/-/-	0.030±0.021 / -2.938		-/-/-	0.020±0.015 / 0.369		-/-/-
Double Support (s)	0.403±0.101		-/-/-	0.390±0.050		-/-/-	0.389±0.028		-/-/-	0.403±0.019		-/-/-
CV_Double Support (%)	25.05		-/-/-	12.748		-/-/-	7.191		-/-/-	4.811		-/-/-
Stride Length (m)	1.179±0.068	0.895±0.068	-24.112/0.273/**<0.001**	1.252±0.089	0.932±0.132	-25.529/0.284/**<0.001**	1.104±0.105	0.972±0.081	-11.941/0.206/**<0.001**	1.173±0.148	0.938±0.093	-20.072/0.309/**<0.001**
CV_Stride Length (%)	58	7.56	30.350/-/-	7.084	14.119	99.324/-/-	9.509	8.316	-12.544/-/-	12.601	9.865	-21.710/-/-
B.I./Symmetry Stride Length	0.137±0.040 / -6.044		-/-/-	0.149±0.069 / -10.664		-/-/-	0.067±0.051 / -7.140		-/-/-	0.123±0.056 / -8.190		-/-/-
Stride Speed (m/s)	0.851±0.050	0.669±0.077	-21.434/-0.104/**<0.001**	0.931±0.078	0.695±0.097	-25.314/0.259/**<0.001**	0.796±0.073	0.704±0.052	-11.503/0.076/**<0.001**	0.833±0.103	0.671±0.064	-19.453/0.219/**<0.001**
CV_Stride Speed (%)	5831	11.518	97.526/-/-	8.327	13.894	66.841/-/-	9.159	7.378	-19.449/-/-	12.409	9.611	-22.549/-/-
B.I./Symmetry Stride Speed	0.126±0.053 / -18.524		-/-/-	0.147±0.072 / -22.033		-/-/-	0.065±0.050 / -7.272		-/-/-	0.121±0.059 / -14.342		-/-/-
Clearance (m)	0.034±0.008	0.013±0.005	-61.914/0.138/**<0.001**	0.060±0.016	0.023±0.006	-61.380/0.186/**<0.001**	0.036±0.012	0.022±0.006	-40.290/0.341/**<0.001**	0.030±0.009	0.019±0.005	-37.929/0.229/**<0.001**
CV_Clearance (%)	22889	41.738	82.348/-/-	26.463	26.497	0.130/-/-	32.459	25.341	-21.930/-/-	28.904	27.332	-5.438/-/-
B.I./Symmetry Clearance	0.453±0.166 / -42.273		-/-/-	0.432±0.144 / -33.229		-/-/-	0.254±0.142 / -38.919		-/-/-	0.241±0.148 / -49.557		-/-/-
Relative Stance Phase (%)	63.918±0.782	64.597±6.306	1.063/-0.246/0.550	64.489±0.550	64.337±2.966	-0.236/0.099/0.777	64.596±1.088	63.146±1.541	-2.246/-0.184/**<0.001**	64.986±0.695	63.359±0.840	-2.504/-0.220/**<0.001**
CV_Relative Stance Phase (%)	1223	9.761	697.930/-/-	0.852	4.61	441.018/-/-	1.685	2.44	44.828/-/-	1.07	1.326	23.977/-/-
B.I./Symmetry Relative St. Ph.	0.023±0.039 / 37.935		-/-/-	0.019±0.012 / 20.887		-/-/-	0.017±0.009 / 12.210		-/-/-	0.013±0.009 / 8.639		-/-/-
	5th SESSION (18/05/16)			**6th SESSION (13/06/16)**			**7th SESSION (30/06/16)**			**8th SESSION (23/09/16)**		
Parameters	**R**	**L**	**Mean Diff. (%) / Paerson's r / p-value**	**R**	**L**	**Mean Diff. (%) / Paerson's r / p-value**	**R**	**L**	**Mean Diff. (%) / Paerson's r / p-value**	**R**	**L**	**Mean Diff. (%) / Paerson's r / p-value**
GCT (s)	1.387±0.036	1.383±0.027	-0.272/0.088/0.637	1.464±0.049	1.455±0.048	-0.602/0.799/0.471	1.396±0.032	1.390±0.030	-0.385/0.667/0.495	1.365±0.054	1.360±0.047	-0.315/0.886/0.736
CV_GCT (%)	2.618	1.922	-26.577/-/-	3.343	3.316	-0.800/-/-	2.317	2.169	-6.386/-/-	3.96	3.467	-12.448/-/-
B.I./Symmetry_GCT	0.012±0.009 / 0.502		-/-/-	0.008±0.008 / 0.018		-/-/-	0.006±0.007 / 0.106		-/-/-	0.006±0.007 / 0.361		-/-/-
Stance Phase (s)	0.909±0.029	0.878±0.023	-3.380/-0.080/**<0.001**	0.964±0.048	0.936±0.044	-2.845/0.755/**0.021**	0.920±0.024	0.882±0.025	-4.079/0.447/**<0.001**	0.890±0.042	0.866±0.029	-2.705/0.691/**0.010**
CV_Stance Phase (%)	3.209	2.596	-19.102/-/-	5.011	4.689	-6.423/-/-	2.612	2.864	9.676/-/-	4.754	3.307	-30.437/-/-
B.I./Symmetry Stance Phase	0.022±0.016 / -0.487		-/-/-	0.016±0.015 / -0.943		-/-/-	0.021±0.014 / -0.500		-/-/-	0.015±0.015 / 0.117		-/-/-
Swing Phase (s)	0.479±0.015	0.505±0.019	5.629/0.353/**<0.001**	0.500±0.011	0.519±0.011	3.721/0.220/**<0.001**	0.476±0.016	0.508±0.015	6.753/0.305/**<0.001**	0.474±0.017	0.494±0.025	4.169/0.643/**<0.001**
CV_Swing Phase (%)	3.03	3.694	21.888/-/-	2.229	2.2	-1.276/-/-	3.393	2.955	-12.925/-/-	3.51	4.96	41.304/-/-
B.I./Symmetry Swing Phase	0.028±0.017 / -0.533		-/-/-	0.018±0.014 / 2.916		-/-/-	0.033±0.018 / -0.373		-/-/-	0.022±0.017 / -0.231		-/-/-
Double Support (s)	0.405±0.026		-/-/-	0.442±0.039		-/-/-	0.413±0.021		-/-/-	0.398±0.024		-/-/-
CV_Double Support (%)	6.361		-/-/-	8.796		-/-/-	5.063		-/-/-	6.156		-/-/-
Stride Length (m)	1.054±0.149	0.994±0.113	-5.708/0.481/0.073	1.276±0.053	1.071±0.052	-16.035/0.412/**<0.001**	1.035±0.133	0.971±0.061	-6.174/0.672/**0.017**	1.043±0.130	0.947±0.082	-9.197/0.626/**0.001**
CV_Stride Length (%)	14.1	11.348	-19.513/-/-	4.182	4.816	15.152/-/-	12.833	6.274	-51.111/-/-	12.472	8.659	-30.573/-/-
B.I./Symmetry Stride Length	0.058±0.044 / -9.969		-/-/-	0.087±0.025 / -0.136		-/-/-	0.041±0.036 / -3.865		-/-/-	0.053±0.040 / -6.179		-/-/-
Stride Speed (m/s)	0.759±0.101	0.718±0.076	-5.419/0.450/0.072	0.872±0.043	0.737±0.042	-15.516/0.432/**<0.001**	0.741±0.086	0.698±0.038	-5.741/0.582/**0.014**	0.763±0.077	0.696±0.048	-8.831/0.380/**<0.001**
CV_Stride Speed (%)	13.364	10.643	-20.355/-/-	4.928	5.693	15.516/-/-	11.635	5.454	-53.128/-/-	10.069	6.95	-30.976/-/-
B.I./Symmetry Stride Speed	0.054±0.044 / -15.909		-/-/-	0.084±0.029 / -6.925		-/-/-	0.039±0.036 / -4.329		-/-/-	0.052±0.041 / -7.249		-/-/-
Clearance (m)	0.034±0.006	0.033±0.009	-0.234/-0.126/0.968	0.032±0.007	0.017±0.004	-46.935/0.091/**<0.001**	0.033±0.006	0.018±0.004	-45.135/0.227/**<0.001**	0.031±0.006	0.026±0.010	-13.621/-0.457/**0.046**
CV_Clearance (%)	18.107	26.931	48.738/-/-	22.225	23.492	5.702/-/-	16.748	23.785	42.016/-/-	19.92	36.949	85.485/-/-
B.I./Symmetry Clearance	0.139±0.127 / -45.973		-/-/-	0.303±0.139 / -41.042		-/-/-	0.294±0.115 / -41.001		-/-/-	0.212±0.156 / -64.720		-/-/-
Relative Stance Phase (%)	65.497±0.830	63.463±1.147	-3.106/0.125/**<0.001**	65.805±1.189	64.325±1.066	-2.250/0.524/**<0.001**	65.629±1.817	63.285±0.975	-3.715/-0.033/**<0.001**	65.238±0.792	63.706±0.894	-2.357/-0.307/**<0.001**
CV_Relative Stance Phase (%)	1.268	1.807	42.553/-/-	1.807	1.657	-8.332/-/-	1.249	1.459	16.879/-/-	1.325	1.475	11.373/-/-
B.I./Symmetry Relative St. Ph.	0.016±0.009 / 11.253		-/-/-	0.011±0.008 / 16.152		-/-/-	0.019±0.010 / 8.737		-/-/-	0.013±0.010 / 11.764		-/-/-

2017, © Copyright by authors, Published under agreement with IARIA - www.iaria.org

TABLE II. GAIT METRICS (4 KM/H)

GAIT 4KM/H	1st SESSION (09/01/2016)			2nd SESSION (16/03/16)			3rd SESSION (07/04/2016)			4th SESSION (26/04/16)		
Parameters	**R**	**L**	**Mean Diff. (%) / Paerson's r / p-value**	**R**	**L**	**Mean Diff. (%) / Paerson's r / p-value**	**R**	**L**	**Mean Diff. (%) / Paerson's r / p-value**	**R**	**L**	**Mean Diff. (%) / Paerson's r / p-value**
GCT (s)	1.166±0.024	1.166±0.021	-0.038/0.739/0.943	1.186±0.018	1.180±0.064	-0.479/0.049/0.662	1.216±0.018	1.217±0.016	0.055/0.670/0.879	1.131±0.025	1.131±0.025	0.075/0.939/0.897
CV_GCT (%)	2.097	1.818	-13.271/-/-	1.476	5.465	270.189/-/-	1.441	1.314	-8.842/-/-	2.213	2.242	1.34/-/-
B.I./Symmetry_GCT	0.005±0.005 / 0.239		-/-/-	0.018±0.022 / -3.364		-/-/-	0.004±0.004 / 0.105		-/-/-	0.003±0.002 / -0.026		-/-/-
Stance Phase (s)	0.718±0.020	0.709±0.015	-1.318/0.659/0.056	0.734±0.017	0.770±0.055	4.842/0.374/**0.003**	0.765±0.015	0.745±0.014	-2.686/0.659/**<0.001**	0.705±0.019	0.691±0.018	-2.000/0.814/**0.005**
CV_Stance Phase (%)	2.787	2.141	-23.183/-/-	2.321	7.189	209.778/-/-	2.023	1.828	-9.644/-/-	2.745	2.619	-4.594/-/-
B.I./Symmetry Stance Phase	0.010±0.007 / -0.277		-/-/-	0.033±0.022 / -1.461		-/-/-	0.014±0.007 / -0.423		-/-/-	0.011±0.007 / -0.332		-/-/-
Swing Phase (s)	0.448±0.011	0.457±0.012	2.014/0.429/**0.005**	0.451±0.010	0.410±0.063	-9.141/0.079/**0.002**	0.451±0.009	0.472±0.006	4.708/0.042/**<0.001**	0.426±0.009	0.441±0.009	3.513/0.537/**<0.001**
CV_Swing Phase (%)	2.42	2.604	7.587/-/-	2.319	15.33	561.136/-/-	2.099	1.244	-40.724/-/-	2.169	2.096	-3.359/-/-
B.I./Symmetry Swing Phase	0.014±0.008 / 0.255		-/-/-	0.070±0.066 / -17.715		-/-/-	0.024±0.009 / 1.017		-/-/-	0.018±0.010 / 0.920		-/-/-
Double Support (s)	0.262±0.020		-/-/-	0.320±0.057		-/-/-	0.293±0.016		-/-/-	0.265±0.012		-/-/-
CV_Double Support (%)	7.635		-/-/-	17.798		-/-/-	5.382		-/-/-	4.465		-/-/-
Stride Length (m)	1.298±0.070	1.111±0.063	-14.431/0.532/**<0.001**	1.353±0.057	1.088±0.082	-19.603/0.031/**<0.001**	1.202±0.091	1.058±0.046	-11.932/0.117/**<0.001**	1.171±0.045	0.785±0.163	-32.901/0.478/**<0.001**
CV_Stride Length (%)	5.371	5.626	4.751/-/-	4.185	7.524	79.773/-/-	7.531	4.37	-41.977/-/-	3.843	20.766	440.346/-/-
B.I./Symmetry Stride Length	0.078±0.026 / -4.916		-/-/-	0.109±0.042 / -0.436		-/-/-	0.065±0.036 / -3.413		-/-/-	0.206±0.100 / -26.265		-/-/-
Stride Speed (m/s)	1.114±0.065	0.953±0.044	-14.462/0.388/**<0.001**	1.141±0.045	0.923±0.073	-19.080/-0.043/**<0.001**	0.989±0.077	0.870±0.041	-11.984/0.195/**<0.001**	1.036±0.046	0.693±0.136	-33.120/0.226/**<0.001**
CV_Stride Speed (%)	5.842	4.608	-21.134/-/-	3.936	7.903	100.776/-/-	7.824	4.713	-39.754/-/-	4.416	19.66	345.173/-/-
B.I./Symmetry Stride Speed	0.078±0.028 / -4.885		-/-/-	0.106±0.044 / -12.376		-/-/-	0.066±0.036 / -5.800		-/-/-	0.206±0.100 / -41.100		-/-/-
Clearance (m)	0.048±0.014	0.017±0.006	-63.693/0.062/**<0.001**	0.057±0.010	0.025±0.007	-57.109/-0.166/**<0.001**	0.049±0.014	0.026±0.003	-48.108/-0.080/**<0.001**	0.042±0.006	0.025±0.003	-40.303/0.587/**<0.001**
CV_Clearance (%)	28.276	34.606	22.383/-/-	17.093	29.702	73.763/-/-	27.537	13.102	-52.42/-/-	14.489	13.589	-6.211/-/-
B.I./Symmetry Clearance	0.462±0.154 / -70.054		-/-/-	0.402±0.153 / -35.059		-/-/-	0.299±0.137 / -25.127		-/-/-	0.251±0.061 / -26.089		-/-/-
Relative Stance Phase (%)	61.596±0.793	60.813±0.717	-1.271/0.285/**<0.001**	61.940±0.873	65.335±4.507	5.482/0.284/**0.001**	62.932±0.711	61.207±0.469	-2.740/0.204/**<0.001**	62.354±0.603	61.062±0.456	-2.072/-0.110/**<0.001**
CV_Relative Stance Phase (%)	1.287	1.179	-8.439/-/-	1.409	6.898	389.572/-/-	1.13	0.766	-32.259/-/-	0.967	0.747	-22.797/-/-
B.I./Symmetry Relative St. Ph.	0.008±0.005 / 24.685		-/-/-	0.032±0.026 / 34.111		-/-/-	0.014±0.005 / 15.737		-/-/-	0.011±0.006 / 14.024		-/-/-
Parameters	**5th SESSION (18/05/16)**			**6th SESSION (13/06/16)**			**7th SESSION (30/06/16)**			**8th SESSION (23/09/16)**		
	R	**L**	**Mean Diff. (%) / Paerson's r / p-value**	**R**	**L**	**Mean Diff. (%) / Paerson's r / p-value**	**R**	**L**	**Mean Diff. (%) / Paerson's r / p-value**	**R**	**L**	**Mean Diff. (%) / Paerson's r / p-value**
GCT (s)	1.154±0.017	1.156±0.015	0.194/0.480/0.574	1.292±0.107	1.292±0.109	0.037/0.869/0.986	1.088±0.020	1.088±0.028	0.003/0.659/0.995	1.101±0.022	1.101±0.022	-0.037/0.779/0.937
CV_GCT (%)	1.48	1.264	-14.567/-/-	8.308	8.406	1.183/-/-	1.86	2.596	39.604/-/-	1.969	2.038	3.537/-/-
B.I./Symmetry_GCT	0.005±0.005 / 0.187		-/-/-	0.013±0.016 / -0.076		-/-/-	0.006±0.008 / -0.677		-/-/-	0.005±0.004 / -0.063		-/-/-
Stance Phase (s)	0.726±0.013	0.709±0.013	-2.243/0.202/**<0.001**	0.837±0.087	0.803±0.079	-4.097/0.848/0.102	0.684±0.016	0.660±0.021	-3.539/0.510/**<0.001**	0.689±0.025	0.673±0.018	-2.312/0.653/**0.003**
CV_Stance Phase (%)	1.729	1.81	4.636/-/-	10.33	9.807	-5.06/-/-	2.331	3.174	36.197/-/-	3.691	2.603	-29.462/-/-
B.I./Symmetry Stance Phase	0.013±0.009 / -0.472		-/-/-	0.026±0.022 / -1.084		-/-/-	0.018±0.014 / -0.531		-/-/-	0.015±0.010 / -0.513		-/-/-
Swing Phase (s)	0.428±0.009	0.447±0.006	4.327/0.174/**<0.001**	0.454±0.033	0.489±0.036	7.655/0.377/**<0.001**	0.404±0.006	0.429±0.018	5.993/0.238/**<0.001**	0.412±0.018	0.428±0.008	3.766/0.222/**<0.001**
CV_Swing Phase (%)	2.18	1.407	-35.459/-/-	7.199	7.42	3.059/-/-	1.606	4.247	164.401/-/-	4.264	1.754	-58.853/-/-
B.I./Symmetry Swing Phase	0.021±0.012 / 0.445		-/-/-	0.043±0.029 / 3.476		-/-/-	0.029±0.020 / -2.801		-/-/-	0.023±0.014 / 2.810		-/-/-
Double Support (s)	0.281±0.011		-/-/-	0.349±0.068		-/-/-	0.255±0.020		-/-/-	0.262±0.024		-/-/-
CV_Double Support (%)	3.821		-/-/-	19.603		-/-/-	7.845		-/-/-	9.329		-/-/-
Stride Length (m)	1.178±0.085	1.156±0.076	-1.887/0.303/0.277	1.162±0.105	0.979±0.147	-15.759/-0.192/**<0.001**	0.989±0.047	0.780±0.156	-21.188/0.076/**<0.001**	1.088±0.118	0.952±0.092	-12.496/0.104/**<0.001**
CV_Stride Length (%)	7.255	6.618	-8.78/-/-	9.05	15.056	66.358/-/-	4.744	20.014	321.893/-/-	10.867	9.633	-11.363/-/-
B.I./Symmetry Stride Length	0.032±0.031 / -6.780		-/-/-	0.108±0.066 / -6.536		-/-/-	0.129±0.117 / -25.524		-/-/-	0.084±0.051 / -10.441		-/-/-
Stride Speed (m/s)	1.021±0.068	1.000±0.063	-2.055/0.228/0.206	0.904±0.088	0.768±0.166	-14.967/0.341/**<0.001**	0.910±0.052	0.717±0.145	-21.199/0.143/**<0.001**	0.988±0.101	0.865±0.076	-12.469/-0.116/**<0.001**
CV_Stride Speed (%)	6.633	6.344	-4.363/-/-	9.773	21.578	120.794/-/-	5.675	20.184	255.634/-/-	10.199	8.785	-13.865/-/-
B.I./Symmetry Stride Speed	0.031±0.031 / -9.729		-/-/-	0.107±0.071 / -31.646		-/-/-	0.129±0.117 / -45.932		-/-/-	0.085±0.053 / -10.971		-/-/-
Clearance (m)	0.047±0.008	0.041±0.005	-11.899/-0.405/**0.002**	0.039±0.009	0.030±0.010	-23.242/0.027/**<0.001**	0.040±0.006	0.027±0.009	-34.109/-0.156/**<0.001**	0.034±0.011	0.035±0.010	2.572/-0.404/0.722
CV_Clearance (%)	17.009	12.597	-25.94/-/-	23.676	33.781	42.676/-/-	14.293	35.24	146.549/-/-	31.821	28.428	-10.663/-/-
B.I./Symmetry Clearance	0.104±0.088 / -25.062		-/-/-	0.186±0.135 / -53.894		-/-/-	0.244±0.133 / -72.296		-/-/-	0.207±0.112 / -62.369		-/-/-
Relative Stance Phase (%)	62.898±0.582	61.365±0.529	-2.438/-0.244/**<0.001**	63.303±0.640	60.770±0.635	-4.088/0.172/**<0.001**	62.835±0.462	60.615±1.225	-3.533/-0.098/**<0.001**	62.569±1.641	61.148±0.529	-2.271/0.382/**<0.001**
CV_Relative Stance Phase (%)	0.926	0.862	-6.896/-/-	3.054	2.406	-21.242/-/-	0.735	2.021	174.96/-/-	2.622	0.865	-67.002/-/-
B.I./Symmetry Relative St. Ph.	0.012±0.007 / 10.518		-/-/-	0.023±0.016 / 49.315		-/-/-	0.018±0.011 / 22.814		-/-/-	0.014±0.009 / 32.365		-/-/-

2017, © Copyright by authors, Published under agreement with IARIA - www.iaria.org

TABLE III. GAIT METRICS (6 KM/H)

GAIT 6KM/H	1st SESSION (09/01/2016)			4th SESSION (26/04/16)			5th SESSION (18/05/16)		
Parameters	R	L	Mean Diff. (%) / Paerson's r / p-value	R	L	Mean Diff. (%) / Paerson's r / p-value	R	L	Mean Diff. (%) / Paerson's r / p-value
GCT (s)	0.925±0.016	0.925±0.017	-0.032/-0.148/0.941	0.955±0.010	0.954±0.012	-0.021/0.517/0.935	0.920±0.010	0.920±0.013	0.007/0.708/0.980
CV_GCT (%)	1.747	1.813	3.798/-/-	1.059	1.247	17.766/-/-	1.11	1.449	30.442/-/-
B.I./Symmetry_GCT	0.007±0.011 / -0.072		-/-/-	0.005±0.003 / -0.197		-/-/-	0.004±0.003 / -0.367		-/-/-
Stance Phase (s)	0.546±0.010	0.532±0.013	-2.573/-0.109/**<0.001**	0.571±0.008	0.559±0.010	-2.089/0.347/**<0.001**	0.543±0.010	0.533±0.011	-1.884/0.615/**<0.001**
CV_Stance Phase (%)	1.9	2.438	28.303/-/-	1.381	1.701	23.159/-/-	1.797	2.08	15.741/-/-
B.I./Symmetry Stance Phase	0.016±0.014 / -0.675		-/-/-	0.012±0.007 / -0.476		-/-/-	0.011±0.006 / -0.686		-/-/-
Swing Phase (s)	0.380±0.012	0.393±0.013	3.619/0.043/**<0.001**	0.383±0.006	0.395±0.006	3.060/0.269/**<0.001**	0.377±0.005	0.387±0.006	2.731/0.055/**<0.001**
CV_Swing Phase (%)	3.044	3.345	9.914/-/-	1.527	1.611	5.542/-/-	1.216	1.465	20.494/-/-
B.I./Symmetry Swing Phase	0.023±0.015 / -2.649		-/-/-	0.016±0.009 / -0.402		-/-/-	0.015±0.007 / 0.610		-/-/-
Double Support (s)	0.152±0.021		-/-/-	0.176±0.010		-/-/-	0.156±0.011		-/-/-
CV_Double Support (%)	13.648		-/-/-	5.851		-/-/-	7.189		-/-/-
Stride Length (m)	1.346±0.090	1.151±0.190	-14.526/0.280/**<0.001**	1.358±0.042	1.152±0.082	-15.112/0.181/**<0.001**	1.310±0.046	1.232±0.063	-5.954/-0.144/**<0.001**
CV_Stride Length (%)	6.683	16.509	147.047/-/-	3.083	7.159	132.205/-/-	3.501	5.073	44.911/-/-
B.I./Symmetry Stride Length	0.086±0.098 / -26.474		-/-/-	0.083±0.037 / -9.758		-/-/-	0.037±0.025 / -5.618		-/-/-
Stride Speed (m/s)	1.456±0.105	1.244±0.208	-14.519/0.170/**<0.001**	1.422±0.048	1.208±0.090	-15.082/0.288/**<0.001**	1.424±0.048	1.339±0.065	-5.963/-0.283/**<0.001**
CV_Stride Speed (%)	7.238	16.686	130.552/-/-	3.368	7.424	120.39/-/-	3.353	4.829	44.027/-/-
B.I./Symmetry Stride Speed	0.089±0.098 / -35.941		-/-/-	0.083±0.037 / -15.383		-/-/-	0.038±0.024 / -9.582		-/-/-
Clearance (m)	0.066±0.014	0.032±0.011	-51.184/0.453/**<0.001**	0.057±0.009	0.033±0.006	-42.273/-0.115/**<0.001**	0.058±0.007	0.047±0.008	-18.035/-0.027/**<0.001**
CV_Clearance (%)	20.361	35.015	71.97/-/-	15.214	19.4	27.513/-/-	11.6	16.631	43.362/-/-
B.I./Symmetry Clearance	0.354±0.130 / -80.517		-/-/-	0.268±0.115 / -45.027		-/-/-	0.115±0.090 / -39.151		-/-/-
Relative Stance Phase (%)	58.973±0.821	57.473±1.093	-2.544/0.105/**<0.001**	59.841±0.481	58.603±0.541	-2.070/0.065/**<0.001**	59.018±0.559	57.902±0.566	-1.892/0.193/**<0.001**
CV_Relative Stance Phase (%)	1.393	1.902	36.54/-/-	0.804	0.922	14.776/-/-	0.947	0.978	3.177/-/-
B.I./Symmetry Relative St. Ph.	0.015±0.009 / 77.317		-/-/-	0.011±0.006 / 28.012		-/-/-	0.010±0.005 / 39.871		-/-/-

Parameters	6th SESSION (13/06/16)			7th SESSION (30/06/16)			8th SESSION (23/09/16)		
	R	L	Mean Diff. (%) / Paerson's r / p-value	R	L	Mean Diff. (%) / Paerson's r / p-value	R	L	Mean Diff. (%) / Paerson's r / p-value
GCT (s)	0.900±0.008	0.900±0.011	-0.003/0.528/0.989	0.886±0.010	0.887±0.028	0.037/0.335/0.944	0.901±0.061	0.925±0.030	2.617/0.348/**0.029**
CV_GCT (%)	0.917	1.169	27.422/-/-	1.098	3.192	190.574/-/-	6.766	3.296	-51.281/-/-
B.I./Symmetry_GCT	0.004±0.003 / -0.279		-/-/-	0.008±0.013 / -2.362		-/-/-	0.018±0.032 / 3.850		-/-/-
Stance Phase (s)	0.535±0.008	0.518±0.010	-3.276/0.233/**<0.001**	0.524±0.007	0.509±0.022	-2.982/0.261/**<0.001**	0.549±0.019	0.538±0.021	-1.914/0.856/**0.021**
CV_Stance Phase (%)	1.51	1.938	28.318/-/-	1.415	4.395	210.523/-/-	3.536	3.956	11.871/-/-
B.I./Symmetry Stance Phase	0.017±0.010 / -0.855		-/-/-	0.017±0.021 / -1.357		-/-/-	0.012±0.008 / -0.713		-/-/-
Swing Phase (s)	0.365±0.007	0.383±0.006	4.796/0.020/**<0.001**	0.362±0.006	0.378±0.027	4.407/0.081/**<0.001**	0.352±0.057	0.387±0.012	9.670/0.041/**<0.001**
CV_Swing Phase (%)	1.806	1.653	-8.436/-/-	1.576	7.054	347.579/-/-	16.272	3.169	-80.525/-/-
B.I./Symmetry Swing Phase	0.024±0.010 / -0.267		-/-/-	0.022±0.031 / -10.758		-/-/-	0.054±0.099 / 0.669		-/-/-
Double Support (s)	0.153±0.010		-/-/-	0.146±0.023		-/-/-	0.163±0.013		-/-/-
CV_Double Support (%)	6.848		-/-/-	15.677		-/-/-	7.775		-/-/-
Stride Length (m)	1.301±0.030	1.202±0.050	-7.566/0.465/**<0.001**	1.211±0.051	0.786±0.165	-35.136/0.176/**<0.001**	1.261±0.060	0.898±0.130	-28.778/0.414/**<0.001**
CV_Stride Length (%)	2.341	4.161	77.771/-/-	4.233	20.979	395.61/-/-	4.734	14.437	204.957/-/-
B.I./Symmetry Stride Length	0.040±0.019 / -4.293		-/-/-	0.221±0.098 / -32.612		-/-/-	0.172±0.067 / -19.476		-/-/-
Stride Speed (m/s)	1.445±0.037	1.336±0.055	-7.567/0.478/**<0.001**	1.367±0.056	0.886±0.184	-35.144/0.085/**<0.001**	1.406±0.119	0.970±0.132	-30.982/0.108/**<0.001**
CV_Stride Speed (%)	2.54	4.108	61.72/-/-	4.064	20.764	410.956/-/-	8.435	13.582	61.019/-/-
B.I./Symmetry Stride Speed	0.040±0.018 / -6.307		-/-/-	0.221±0.099 / -52.995		-/-/-	0.185±0.073 / 7.632		-/-/-
Clearance (m)	0.058±0.006	0.041±0.008	-29.571/0.120/**<0.001**	0.048±0.004	0.037±0.013	-24.058/0.011/**<0.001**	0.045±0.006	0.058±0.014	28.036/-0.204/**<0.001**
CV_Clearance (%)	10.61	19.632	85.033/-/-	9.04	35.723	295.162/-/-	13.914	24.693	77.468/-/-
B.I./Symmetry Clearance	0.181±0.095 / -46.997		-/-/-	0.184±0.122 / -75.838		-/-/-	0.178±0.103 / -55.680		-/-/-
Relative Stance Phase (%)	59.456±0.663	57.508±0.692	-3.276/-0.073/**<0.001**	59.145±0.489	57.380±2.216	-2.990/0.038/**<0.001**	61.147±4.604	58.188±0.761	-4.839/0.017/**<0.001**
CV_Relative Stance Phase (%)	1.116	1.203	7.823/-/-	0.826	3.861	367.397/-/-	7.53	1.309	-82.621/-/-
B.I./Symmetry Relative St. Ph.	0.017±0.008 / 36.958		-/-/-	0.016±0.020 / 80.676		-/-/-	0.024±0.035 / 39.576		-/-/-

2017, © Copyright by authors, Published under agreement with IARIA - www.iaria.org

TABLE IV. KINEMATICS METRICS - RANGE OF MOTION

		1st SESSION (09/01/2016)			2nd SESSION (16/03/16)			3rd SESSION (07/04/2016)			4th SESSION (26/04/16)		
	Parameters	R	L	Mean Diff. (%)	R	L	Mean Diff. (%)	R	L	Mean Diff. (%)	R	L	Mean Diff. (%)
Hamstring Curl	ROM X-axis	-	82.641±2.737	-	118.172±1.482	67.951±7.716	-73.908	111.836±3.241	91.923±1.286	-21.662	112.139±8.342	107.131±1.703	-4.674
	ROM Y-axis	-	15.442±1.372	-	9.575±1.286	9.020±1.303	-6.152	8.221±1.204	5.572±0.663	-47.551	9.983±2.843	8.373±0.962	-19.236
	ROM Z-axis	-	27.078±0.947	-	14.677±1.592	13.410±1.025	-9.445	13.657±1.141	9.230±1.027	-47.965	14.078±1.083	15.175±1.587	7.229
Flexion - Extension	ROM X-axis	-	-	-	122.970±1.671	100.828±0.665	-21.961	128.016±1.655	110.347±1.379	-16.012	130.550±1.313	52.832±7.771	-147.101
	ROM Y-axis	-	-	-	11.910±1.204	5.595±0.759	-112.887	26.833±1.859	18.286±1.322	-46.742	39.836±1.530	21.647±1.962	-84.02
	ROM Z-axis	-	-	-	13.209±1.298	5.724±0.264	-130.751	13.983±1.566	9.421±0.548	-48.429	13.371±1.222	10.190±0.951	-31.214
Squat	ROM X-axis	85.137±1.556	77.938±1.957	-9.236	-	-	-	-	-	-	93.786±23.775	84.844±20.745	-10.539
	ROM Y-axis	13.301±1.066	14.791±1.132	10.074	-	-	-	-	-	-	7.775±1.439	10.368±1.331	25.012
	ROM Z-axis	20.824±1.257	7.271±1.185	-186.408	-	-	-	-	-	-	20.032±4.139	13.505±1.464	-48.333
Gait - 3km/h	ROM X-axis	64.315±2.097	69.389±1.564	7.313	66.998±1.193	59.320±2.845	-12.944	61.618±1.524	60.458±1.856	-1.918	61.569±1.959	62.875±2.153	2.077
	ROM Y-axis	15.569±0.946	32.374±1.626	51.909	9.667±1.347	7.738±0.923	-24.937	14.965±1.142	7.379±0.790	-102.789	12.786±1.458	7.635±1.020	-67.455
	ROM Z-axis	37.565±101.720	42.273±96.859	11.137	13.050±1.545	10.121±1.170	-28.935	56.325±127.917	54.878±118.030	-2.637	61.721±121.070	44.364±106.139	-39.124
Gait - 4km/h	ROM X-axis	69.369±1.943	62.329±2.195	-11.294	74.203±1.353	70.244±1.834	-5.636	75.348±1.404	68.997±2.261	-9.205	66.626±1.461	63.836±2.433	-4.37
	ROM Y-axis	21.117±1.394	27.893±1.524	24.292	18.488±1.456	11.364±1.093	-62.685	13.404±1.347	9.797±1.206	-36.828	12.007±1.173	9.230±1.234	-30.097
	ROM Z-axis	43.085±111.755	16.996±1.488	-153.494	37.707±71.355	97.983±170.923	61.517	29.822±62.300	51.402±114.929	41.982	70.068±117.421	86.848±137.315	19.321
Gait - 6km/h	ROM X-axis	74.423±2.902	74.423±2.902	0	-	-	-	-	-	-	62.210±3.627	62.975±2.834	1.215
	ROM Y-axis	16.550±1.099	16.578±1.087	0.167	-	-	-	-	-	-	10.882±2.085	11.073±2.634	1.719
	ROM Z-axis	0.253±0.030	0.485±0.053	47.949	-	-	-	-	-	-	0.353±0.034	0.260±0.043	-35.844

		5th SESSION (18/05/16)			6th SESSION (13/06/16)			7th SESSION (30/06/16)			8th SESSION (23/09/16)		
	Parameters	R	L	Mean Diff. (%)	R	L	Mean Diff. (%)	R	L	Mean Diff. (%)	R	L	Mean Diff. (%)
Hamstring Curl	ROM X-axis	117.846±3.826	103.190±1.148	-14.203	122.307±1.865	97.093±3.927	-25.968	124.366±4.442	107.887±2.183	-15.275	108.661±3.817	104.718±2.630	-3.766
	ROM Y-axis	13.977±1.564	6.199±0.885	-125.463	16.278±1.389	22.596±2.363	27.964	12.218±1.921	5.345±0.996	-128.599	8.360±0.624	12.970±3.672	35.544
	ROM Z-axis	12.930±1.294	10.522±1.073	-22.887	8.931±1.843	12.545±1.539	28.806	11.295±1.444	10.343±1.556	-9.203	15.470±2.234	9.770±1.790	-58.332
Flexion - Extension	ROM X-axis	131.971±0.905	117.418±18.965	-12.393	131.493±0.937	116.473±20.045	-12.896	118.717±30.309	114.172±0.779	-3.981	129.839±1.810	125.422±2.211	-3.522
	ROM Y-axis	38.799±1.058	8.743±2.887	-343.755	52.276±0.934	14.720±1.769	-255.133	36.921±8.907	20.145±0.750	-83.279	29.963±1.160	14.866±2.571	-101.554
	ROM Z-axis	14.060±1.322	24.059±5.151	41.56	10.785±1.602	20.287±3.439	46.836	10.558±2.134	7.827±1.082	-34.894	22.439±1.579	50.844±5.072	55.867
Squat	ROM X-axis	101.020±1.566	95.359±1.633	-5.937	107.942±2.646	105.372±1.911	-2.439	112.705±1.005	104.399±1.400	-7.956	113.666±2.134	111.234±1.787	-2.187
	ROM Y-axis	6.575±0.659	11.905±1.118	44.773	11.268±1.075	15.684±0.878	28.156	7.939±0.644	11.326±0.903	29.911	11.578±0.362	13.253±0.599	12.641
	ROM Z-axis	21.238±0.862	9.852±1.292	-115.58	35.327±3.577	9.488±1.452	-272.322	24.207±0.927	6.238±0.587	-288.068	26.917±1.753	30.551±1.283	11.894
Gait - 3km/h	ROM X-axis	60.579±2.259	66.247±2.637	8.555	72.426±1.491	70.794±1.900	-2.306	55.414±2.689	51.661±1.485	-7.265	53.176±1.138	51.526±1.278	-3.202
	ROM Y-axis	10.054±0.959	5.911±0.841	-70.108	14.852±0.777	10.702±1.046	-38.774	8.995±1.346	9.393±0.985	4.244	15.110±1.223	11.166±0.719	-35.314
	ROM Z-axis	11.962±1.459	12.904±1.416	7.3	41.660±88.841	56.070±122.277	25.701	33.680±68.179	41.548±102.441	18.937	38.943±93.873	33.845±76.223	-15.063
Gait - 4km/h	ROM X-axis	63.176±1.906	64.103±1.491	1.445	70.553±1.306	70.143±2.085	-0.584	54.296±1.555	67.237±2.838	19.246	57.188±3.058	55.030±2.635	-3.922
	ROM Y-axis	10.539±0.977	7.519±0.575	-40.174	15.843±1.062	11.567±1.421	-36.964	10.335±0.930	13.904±1.465	25.668	15.116±1.227	12.386±1.086	-22.043
	ROM Z-axis	52.219±111.187	65.127±130.501	19.821	31.082±73.570	60.803±106.116	48.88	65.515±107.396	89.535±136.189	26.827	65.964±111.284	92.638±143.424	28.794
Gait - 6km/h	ROM X-axis	67.009±1.945	67.382±1.628	0.553	70.296±3.683	70.785±3.341	0.69	81.588±2.609	81.360±2.792	-0.281	67.352±4.163	67.285±4.439	-0.1
	ROM Y-axis	8.530±2.462	9.406±1.720	9.31	14.178±2.371	14.433±1.652	1.765	23.515±2.517	23.850±3.276	1.404	15.568±2.225	16.043±2.186	2.966
	ROM Z-axis	0.288±0.039	0.397±0.037	27.51	0.318±0.040	0.372±0.022	14.394	0.380±0.054	0.303±0.031	-25.552	0.389±0.043	0.363±0.045	-7.404

2017, © Copyright by authors, Published under agreement with IARIA - www.iaria.org

variance (at 4 km/h), and level of skew and energy (at 6 km/h). Analyzing the decomposed acceleration around the three components, other useful metrics are provided by the peak-to-peak amplitude/CV around the vertical axis (for both 3-4 km/h), standard deviation over the sagittal plane (at 3 km/h), mean around the x-axis (at 4 km/h), and the peak-to-peak amplitude over the x-axis, and the y-axis maximum (at 6 km/h). Finally, also the angular rate over its three components shows some trends. For example, the peak-to-peak amplitude over the sagittal axis is present at every speed, along with the y-axis standard deviation and PP at 4 km/h. The minimum over the x-axis is a parameter showing specific trends at every speed as well, together with the x-axis maximum/y-axis minimum at 3 km/h.

It is also evident how some of those features present a monotonic trend after the second session, showing a relevant performance gap between the first two sessions, due to the impact of the surgery event on the patient's mobility.

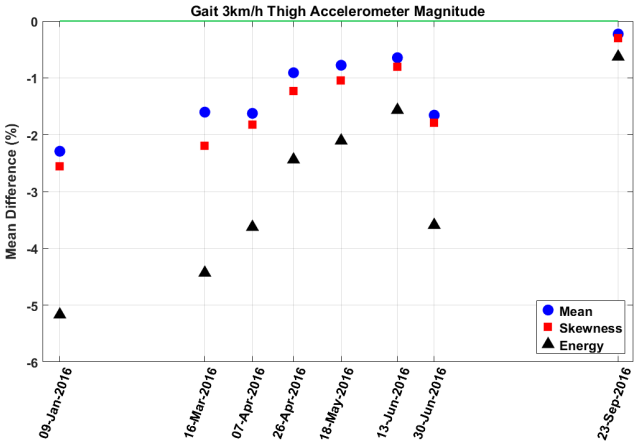


Figure 8. Mean difference for different statistical parameters in the gait scenario (3 km/h) showing the trends of progress during rehabilitation. Mean/skewness/energy for the acceleration thigh magnitude are shown

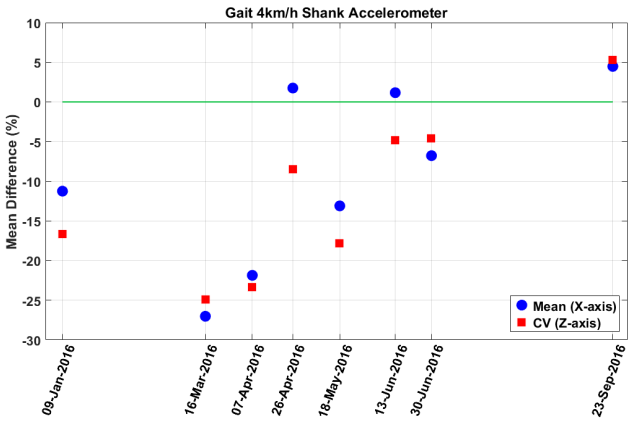


Figure 9. Mean difference for different statistical parameters in the gait scenario (4 km/h) showing the trends of progress during rehabilitation. Mean/CV for the acceleration shank x-, z-axis are shown

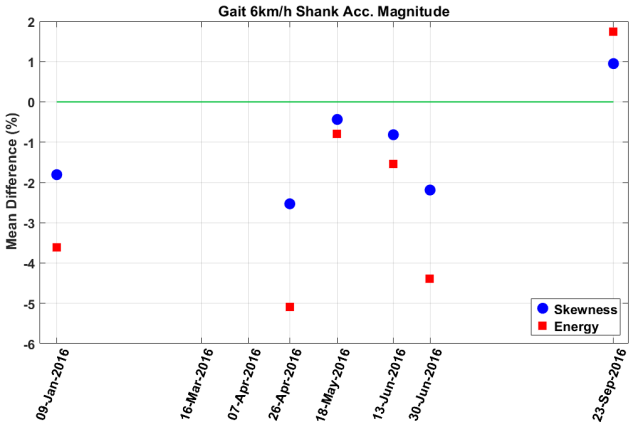


Figure 10. Mean difference for different statistical parameters in the gait scenario (6 km/h) showing the trends of progress during rehabilitation. Skewness/energy for the acceleration shank magnitude are shown

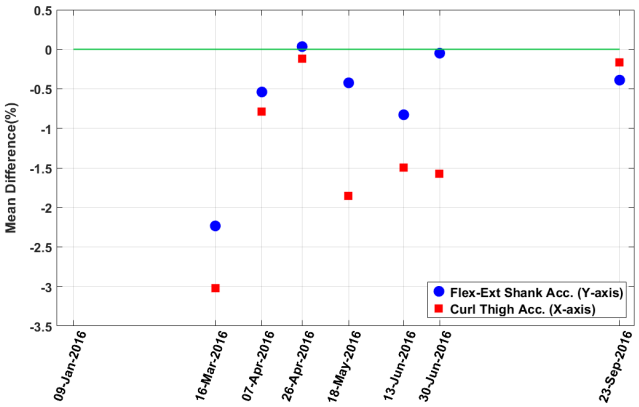


Figure 11. Mean difference for autocorrelation values in different scenarios showing the trends of progress during rehabilitation. X-axis thigh acceleration/y-axis shank acceleration for the hamstring curl/flexion-extension are shown

Finally, biased autocorrelation (e.g., the amplitude of the first dominant) has also been considered for all the scenarios (Figure 11). It has been calculated on both acceleration and angular rate from thigh and shank, but the computation has not been carried out on the single repetitions/strides but on the whole recorded session. In the hamstring curl test, autocorrelation on the x-axis of both acceleration and angular rate signals shows specific trends. On the other side, only y-axis autocorrelation for the shank acceleration was helpful in the flexion/extension scenario. Moreover, x-, z-axis autocorrelation in the shank acceleration and y-, z-axis autocorrelation in the thigh angular rate presented an observable trend in the half squat test. Eventually, in the walking scenario, the z-axis autocorrelation in the acceleration (at 3-4 km/h) was detected as for the thigh, while the x-axis autocorrelation for the gyro (4 km/h) and the y-axis autocorrelation in the acceleration (at 6 km/h) were noticed on the shank.

2017, © Copyright by authors, Published under agreement with IARIA - www.iaria.org

iii. Kinematics Features

Finally, the kinematic features described in Section IV have been calculated as well for each repetition/stride for all the four WIMUs adopted and for both acceleration and angular rate signals. Results are summarized for all the scenarios in the tables in the Appendix and discussed below. The table related to the ROM calculation is also integrated in the paper as an example (Table IV).

In the hamstring curl scenario, most of the detected features are present on the sagittal plane, given that the movement is mostly performed on this plane. The ROM over the x-axis is a clear example, while thigh and shank present similar results related to all the jerk-measures along the y-axis, and the fluency metrics over the sagittal plane. Moreover, the shank shows additional helpful parameters in the RANG and the vertical acceleration feature.

Similar results are shown for the flexion/extension scenario. X-axis ROM is one of the key metrics for highlighting patient progress, together with RANG shared by both thigh and shank. The thigh is also characterized by other metrics (in particular, jerk-measures N_MSJ, IAJ, and M_MAJ over both the x-, z-axis), while the metrics associated to the shank can be reduced to most of the jerk-measures and fluency both along the z-axis, as well as KV.

In the half squat test, again, ROM over the x-axis proved to be a helpful metrics, together with all the jerk-measures over the y-axis (z-axis) obtained from the thigh (shank). Additional metrics were detected in the z-axis stability for the thigh, and the RANG and vertical velocity for the shank. Results for these three scenarios are illustrated in Figure 12.

Gait tests have been also analyzed by using the kinematics variables. While ROM is not always showing particular trends (except at high speed over the x- and z-axis), there is a certain similarity among the feature detection at different speeds. For example, all jerk-measures over the anteroposterior axis on the thigh present clear convergence trends for every speed, while RANG and fluency over the thigh y-axis are more evident at 4-6 km/h, and stability is instead highlighted at slower speeds (3-4 km/h). Likewise, regarding the shank, jerk-measures are highly informative at every speed, especially over the y-axis, even though N_MSJ and N_MAJ trends are also clear over the x-axis. Finally, whereas vertical velocity and z-axis fluency metrics show clear indications at 6 km/h, KV is more impactful at slower speeds (3-4 km/h). Some of the results for the walking scenarios are illustrated in Figure 13.

Regularity measures have been also obtained for all the scenarios (Figures 14-16). While y-axis regularity and x-axis one were observed in the shank acceleration and angular rate, respectively, during the hamstring curl, only the thigh y-axis regularity over the gyroscope was reliable for the flexion/extension. Regularity calculated in the squat scenario provides indications when obtained from the thigh data, in particular the y-axis acceleration, and the x-, y-axis of the angular rate. Conversely, in the gait test, the regularity obtained from the shank are more informative, in particular the acceleration y-, z-axis (for walking at 3 and 6 km/h respectively) and the gyro z-axis (when walking at 4km/h).

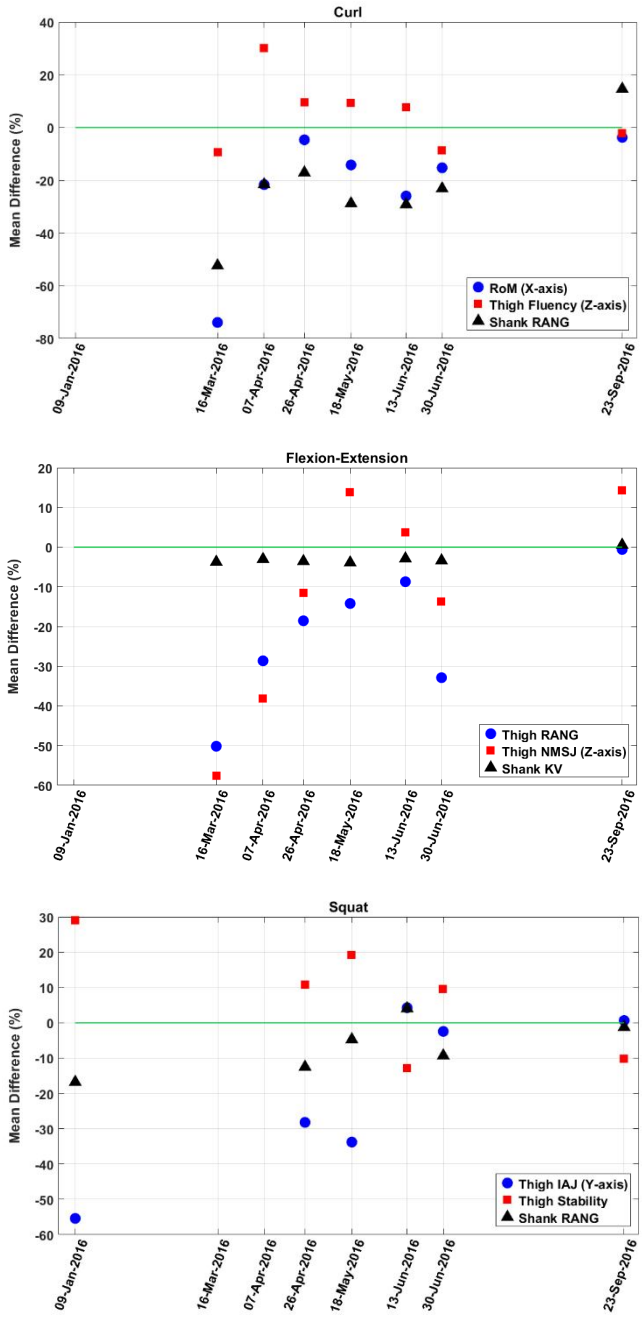


Figure 12. Mean difference for different kinematics variables in a number of scenarios showing the trends of progress during rehabilitation. ROM/Fluency/RANG on the shank/thigh for the hamstring curl are on the top, RANG/NMSJ/KV on the shank/thigh for the flexion/extension in the centre, IAJ/Stability/RANG on the shank/thigh for the squat on the bottom

2017, © Copyright by authors, Published under agreement with IARIA - www.iaria.org

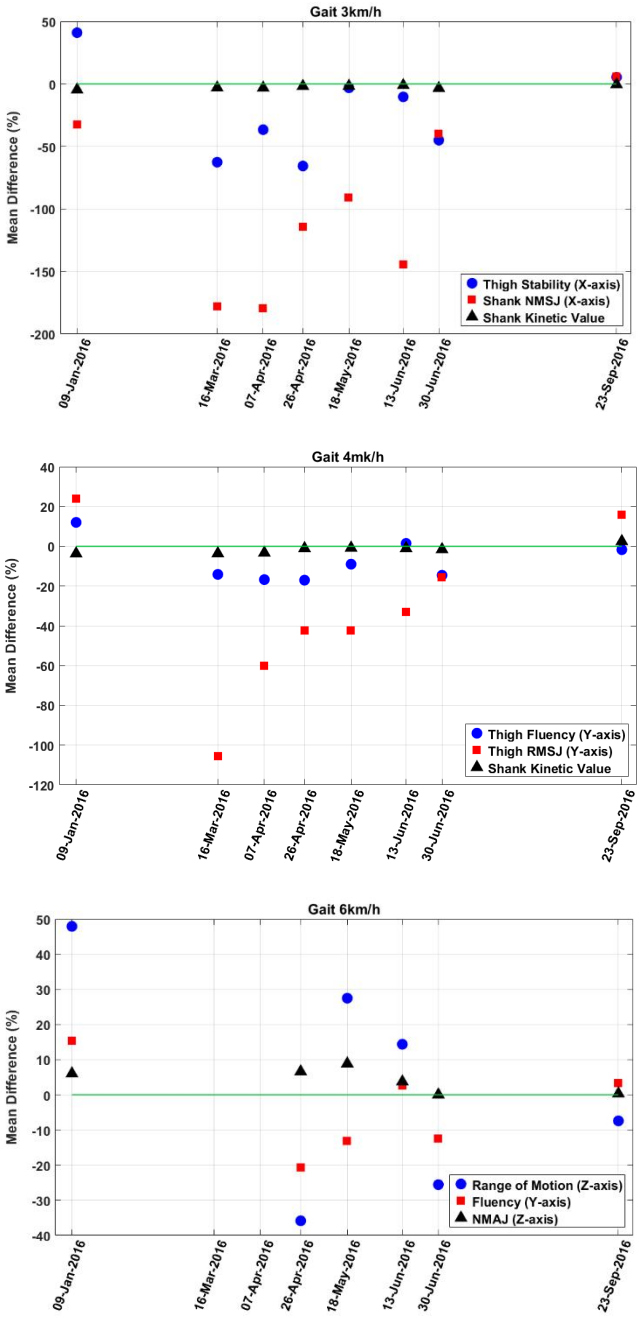


Figure 13. Mean difference for different kinematics variables in a number of scenarios showing the trends of progress during rehabilitation. Stability/NMSJ/KV on the shank/thigh for 3 km/h gait are on the top, Fluency/RMSJ/KV on the shank/thigh for 4 km/h gait in the centre, ROM/Fluency/NMAJ on the shank/thigh for 6 km/h on the bottom

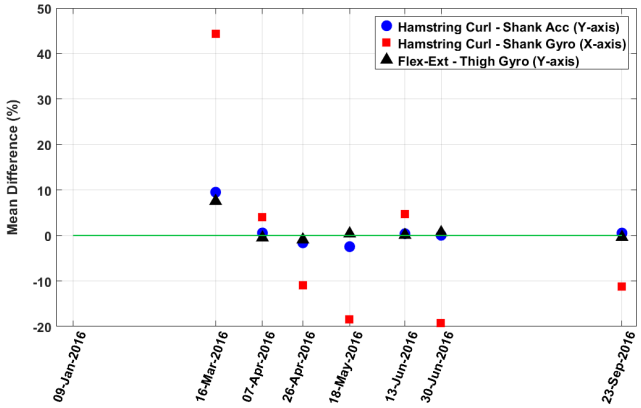


Figure 14. Mean difference for regularity variables in a number of scenarios showing the trends of progress during rehabilitation. Y-axis on the shank acceleration for hamstring curl, x-axis on the gyro shank for hamstring curl, and y-axis on the gyro thigh for flexion/extension are shown. Each variable is normalized according to its mean value for visualization purposes

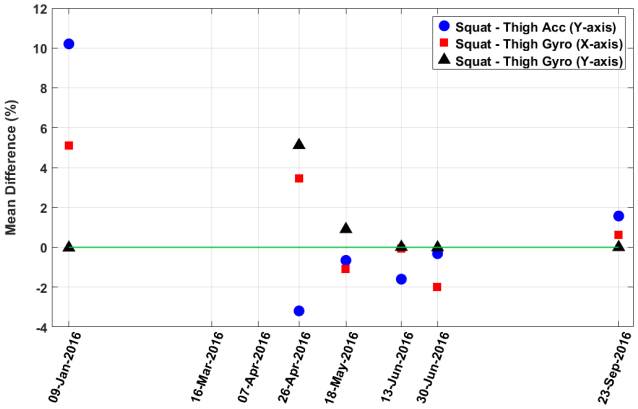


Figure 15. Mean difference for regularity variables for half squat scenario showing the trends of progress during rehabilitation. Y-axis on the thigh acceleration, x-axis on the gyro thigh, and y-axis on the gyro thigh are shown. Each variable is normalized according to its mean value for visualization purposes

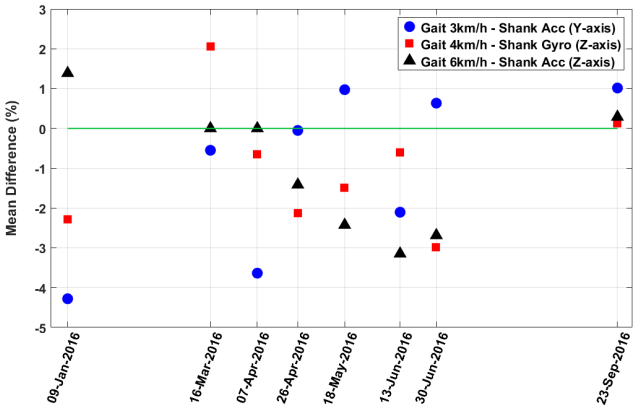


Figure 16. Mean difference for regularity variables for gait scenario showing the trends of progress during rehabilitation. Y-axis on the shank acceleration, z-axis on the gyro shank, and z-axis on the shank acceleration are shown. Each variable is normalized according to its mean value for visualization purposes

2017, © Copyright by authors, Published under agreement with IARIA - www.iaria.org

To summarize, this work analyzed the body-worn inertial data collected from a patient over the course of rehabilitation defining which features and metrics are the most sensitive for better understanding and monitoring patient's progress in several test. As per gait metrics, temporal variables (and, in particular their CV) can be useful at slower speeds, while clearance-related parameters have higher impact at faster speeds. However, those metrics cannot be adopted for other types of movements which, in turn, can be described through statistical and kinematics variables. Given the movement typically performed on a 2D plane, hamstring curl and flexion/extension show a number of usable metrics obtained from both acceleration and angular rate of the shank and thigh, while the squat is characterized by less features. Probably, this can be due to the fact that the squat test, differently from the other exercises, requires a simultaneous movement of both legs which may involve some compensation between the injured and uninjured limbs not evident when only one leg is involved in the test. Gait can be also illustrated through metrics extrapolated from the inertial data collected on the shank, especially when associated to the sagittal plane. Finally, kinematics variables, in particular ROM, RANG, jerk-based measures, fluency, KV and stability, have proved their sensitivity for a different number of scenarios.

Even though this paper reviewed a large number of features, there remain opportunities for further analysis. This work has not considered frequency-domain, entropy-based, or informatics-theoretic parameters. These parameters should be also evaluated in future studies with the aim of developing a complete framework for collecting data and monitoring patients' progress over the course of rehabilitation. Moreover, as only one subject has been studied for the present proof of concept study, an enhanced number of athletes, with homogeneous characteristics, will also be tested in future so as to have a more robust base for the study and further validate the drawn conclusions in statistical terms. Additional clinical trials are, thus, currently being planned.

VI. CONCLUSIONS

This work presented a wearable inertial system equipped with both hardware and time-domain data analytics for an objective assessment of lower-limbs in patients over the course of rehabilitation. The analysis involved body-worn inertial data collected from thighs and shanks, and the implementation of a number of gait-related, statistical, and kinematics features available in literature, with the ultimate goal of defining which metrics are the most sensitive for better understanding and monitoring patient's progress. Accurate results have been achieved in a number of scenarios.

An enhanced number of subjects, with homogeneous characteristics, will also be tested in future so as to have a more robust base for the study and further validate the drawn conclusions in statistical terms. Additional clinical trials are, thus, currently being planned.

However, the present study proved that inertial-based time-domain features can be used for a quantitative biomechanics monitoring and assessment of lower-limbs in different tests over the course of a nine month rehabilitation program, also defining which of those features should be taken into account by clinicians during their analysis.

REFERENCES

[1] S. Tedesco, A. Urru, J. Peckitt, B. O'Flynn, "Wearable inertial sensors as a tool for quantitative assessment of progress during rehabilitation," Int Conf on Global Health Challenges, pp. 56-59, 2016.

[2] R. Bartlett, "Introduction to sports biomechanics: analysing human movement patterns," (2nd ed.) Routledge, London (2007).

[3] http://www.vicon.com/ (accessed 27/02/2017)

[4] http://www.optitrack.com/ (accessed 27/02/2017)

[5] http://www.codamotion.com/ (accessed 27/02/2017)

[6] E. Mirek, M. Rudzińska, A. Szczudlik, ''The assessment of gait disorders in patients with Parkinson's disease using the three-dimensional motion analysis system Vicon,'' Neurol Neurochir Pol., vol. 41, no. 2, pp. 128-133, 2007.

[7] A.D. Segal, M.S. Orendurff, G.K. Klute, M.L. McDowell, J.A. Pecoraro, J. Schofer, J.M. Czerniecki, ''Kinematic and kinetic comparisons of transfemoral amputee gait using C-Leg and Mauch SNS prosthetic knees," J Rehabil Res Dev., vol. 43, no. 7, pp. 857-870, 2006.

[8] S. Lustig, R. A. Magnussen, L. Cheze, P. Neyret, ''The KneeKG system: a review of the literature,'' Knee Surg Sports Traumatol Arthrosc., vol. 20, no. 4, pp. 633-638, 2012.

[9] B. Shabani, D. Bytygi, S. Lustig, L. Cheze, C. Bytygi, P. Neyret, ''Gait knee kinematics after ACL reconstruction: 3D assessment,'' Int Orthopaedics (SICOT), vol. 39, no. 6, pp. 1187-1193, June 2015.

[10] T. Chau, S. Young, S. Redekop, "Managing variability in the summary and comparison of gait data," J Neuroeng Rehabil., vol. 2, no. 22, pp. 1-20, 2005.

[11] A. Castelli, G. Paolini, A. Cereatti, M. Bertoli, U. Della Croce, "Application of a markerless gait analysis methodology in children with cerebral palsy: Preliminary results," Gait & Posture, vol. 42, supp. 2, pp. S4-S5, 2015.

[12] J.F. Item-Glatthorn, N.C. Casartelli, N.A. Maffiuletti, "Reproducibility of gait parameters at different surface inclinations and speeds using an instrumented treadmill system," Gait & Posture, vol. 44, pp. 259–264, 2016.

[13] H.B. Menz, M.D. Latt, A. Tiedemann, M. Mun San Kwan, S.R. Lord, "Reliability of the GAITRite® walkway system for the quantification of temporo-spatial parameters of gait in young and older people," Gait & Posture, vol. 20, no. 1, pp 20–25, 2004.

[14] M. Piirtola, P. Era, "Force platform measurements as predictors of falls among older people – A review," Gerontology, vol. 52, no. 1, pp. 1-16, 2006.

[15] N.J. Collins, D. Misra, D.T. Felson, K.M. Crossley, E.M. Roos, "Measures of knee function," Arthritis Care Res (Hoboken), vol. 63, no. 11, pp. S208–S228, 2011.

2017, © Copyright by authors, Published under agreement with IARIA - www.iaria.org

[16] S. Tilley, N. Thomas, "What knee scoring system?," J. Bone Joint Surgery, pp. 1-4, 2010.

[17] D.T.P. Fong, Y.Y. Chan, "The use of wearable inertial motion sensors in human lower limb biomechanics studies: A systematic review," Sensors, vol. 10, no. 12, pp. 11556-11565, 2010.

[18] J. Barton, A. Gonzalez, J. Buckley, B. O'Flynn, S.C. O'Mathuna, "Design, fabrication and testing of miniaturised wireless inertial measurement units (IMU)," IEEE Electronic Components and Technology Conference (ECTC), pp. 1143-1148, 2007.

[19] M. Walsh, M. O'Grady, M. Dragone, R. Tynan, A. Ruzzelli, J. Barton, B. O'Flynn, G. O'Hare, C. O'Mathuna, "The CLARITY modular ambient health and wellness measurement platform," IEEE Int. Conf. Sensor Technologies and Applications (SENSORCOMM), pp. 577-583, 2010.

[20] D. Kennedy, M. Walsh, B. O'Flynn, "Development of a miniature, low-cost wave measurement solution," IEEE Oceans-St. John's, 2014, pp. 1-6.

[21] B. O'Flynn, J.T. Sanchez, S. Tedesco, B. Downes, J. Connolly, J. Condell, K. Curran, "Novel smart glove technology as a biomechanical monitoring tool," Sensors & Transducers, vol. 193, no. 10, pp. 23-32, Oct. 2015.

[22] N. Ahmad, R. Ariffin, N.M. Khairi, V. Kasi, "Reviews on various inertial measurement unit (IMU) sensor applications," Int J Signal Processing Systems, vol. 1, no. 2, pp. 256-262, 2013.

[23] K. Aminian, B. Najafi, C. Büla, P.F. Leyvraz, P. Robert, "Spatiotemporal parameters of gait measured by an ambulatory system using miniature gyroscopes," J Biomech, vol. 35, pp. 689–699, 2002.

[24] R.E. Mayagoitia, A.V. Nene, P.H. Veltink, "Accelerometer and rate gyroscope measurement of kinematics: an inexpensive alternate to optical motion analysis systems," J Biomech, vol. 35, pp. 537–542, 2002.

[25] A.M. Sabatini, C. Martelloni, S. Scapellato, F. Cavallo, "Assessment of walking features from foot inertial sensing," IEEE Trans. Biomedical Eng., vol. 52, no. 3, pp. 486-494, 2005.

[26] E. Wade, M.J. Mataric, "Design and testing of lightweight inexpensive motion-capture devices with application to clinical gait analysis," Int. Conf. Pervasive Computing Technologies Healthcare, pp. 1-7, April 2009.

[27] L. Atallah, A. Wiik, G. Jones, B. Lo, J. Cobb, A. Amis, G.Z. Yang, "Validation of an ear-worn sensor for gait monitoring using a force-plate instrumented treadmill," Gait & Posture, vol. 35, pp. 674–676, 2012.

[28] S. Kobashi, K. Kawano, Y. Tsumori, S. Yoshiya, Y. Hata, "Wearable joint kinematic monitoring system using inertial and magnetic sensors," IEEE Workshop Robotic Intelligence Informationally Structured Space, pp. 25–29, 2009.

[29] J.C. Van den Noort, V.A. Scholtes, J. Harlaar, "Evaluation of clinical spasticity assessment in cerebral palsy using inertial sensors," Gait & Posture, vol. 30, no. 2, pp. 138–143, 2009.

[30] Y. Guo, D. Wu, G. Liu, G. Zhao, B. Huang, L. Wang, "A low-cost body inertial-sensing network for practical gait discrimination of hemiplegia patients," Telemed J E Health, vol. 18, no. 10, pp. 748-754, 2012.

[31] Y. Guo, G. Zhao, G. Liu, Z. Mei, K. Ivanov, L. Wang, "Balance and knee extensibility evaluation of hemiplegic gait using an inertial body sensor network," BioMedical Engineering OnLine, vol. 12, pp. 83, 2013.

[32] S. Das, L. Trutoiu, A. Murai, D. Alcindor, M. Oh, F. De La Torre, J. Hodgins, "Quantitative measurement of motor symptoms in Parkinson's disease: A study with full-body motion capture data," IEEE Int Conf Eng Med Biol Soc, pp. 6789–6792, 2011.

[33] J.R. Merory, J.E. Wittwer, C.C. Rowe, K.E. Webster, "Quantitative gait analysis in patients with dementia with Lewy bodies and Alzheimer's disease," Gait & Posture, vol. 26, no. 3, pp. 414 –419, 2007.

[34] M. Monda, A. Goldberg, P. Smitham, M. Thornton, J. McCarthy, "Use of inertial measurement units to assess age-related changes in gait kinematics in an active population," J Aging Phys Act, vol. 23, no. 1, pp. 18-23, 2015.

[35] S. Tedesco, A. Urru, A. Clifford, B. O'Flynn, "Experimental validation of the Tyndall portable lower-limb analysis system with wearable inertial sensors," Procedia Engineering, The Engineering of Sport 11, vol. 147, pp. 208-213, 2016.

[36] R. Nerino, L. Contin, A. Tirri, G. Massazza, A. Chimienti, G. Pettiti, N. Cau, V. Cimolin, "An improved solution for knee rehabilitation at home," Int Conf Body Area Networks, pp. 62-68, 2014.

[37] P. Fergus, K. Kafiyat, M. Merabti, A. Taleb-bendiab, A. El Rhalibi, "Remote physiotherapy treatments using wireless body sensor networks," Int Conf Wireless Communications Mobile Computing: Connecting the World Wirelessly, pp. 1191–1197, 2009.

[38] S.L. Han, M.J. Xie, C.C. Chien, Y.C Cheng, C.W. Tsao, "Using MEMS‐based inertial sensor with ankle foot orthosis for telerehabilitation and its clinical evaluation in brain injuries and total knee replacement patients," Microsystem Technologies, vol. 22, no. 3, pp. 625-634, 2016.

[39] O.M. Giggins, K.T. Sweeney, B. Caulfield, "Rehabilitation exercise assessment using inertial sensors: a cross-sectional analytical study," J NeuroEng Rehab, vol. 11, pp. 158, 2014.

[40] P.E. Taylor, G.J. Almeida, T. Kanade, J.K. Hodgins, "Classifying human motion quality for knee osteoarthritis using accelerometers," IEEE Int Conf Eng Med Biol Soc, pp. 339-343, 2010.

[41] P.E. Taylor, G.J. Almeida, J.K. Hodgins, T. Kanade, "Multi-label classification for the analysis of human motion quality," IEEE Int Conf Eng Med Biol Soc, pp. 2214-2218, 2012.

[42] E. Papi, D. Osei-Kuffour, Y.M.A. Chen, A.H. McGregor, "Use of wearable technology for performance assessment: A validation study," Med Eng Phys, vol. 37, no. 7, pp. 698-704, 2015.

[43] G. Fenu, G. Steri, "IMU based post-traumatic rehabilitation assessment," Int. Symp. Applied Sciences in Biomedical and Communication Technologies , pp. 1-5, 2010.

[44] P.C. Chen, C.N. Huang, I.C. Chen, C.T. Chan, "A rehabilitation exercise assessment system based on wearable sensors for knee osteoarthritis," Int Conf Smart Homes Health Telematics, pp. 267-272, 2013.

[45] K.H. Chen, P.C. Chen, K.C. Liu, C.T. Chan, "Wearable sensor-based rehabilitation exercise assessment for knee osteoarthritis," Sensors, vol. 15, no. 2, pp. 4193-4211, 2015.

2017, © Copyright by authors, Published under agreement with IARIA - www.iaria.org

[46] Y.C. Tseng, C.H. Wu, F.J. Wu, C.F. Huang, C.T. King, C.Y. Lin, J.P. Sheu, C.Y. Chen, C.Y. Lo, C.W. Yang, C.W. Deng, "A wireless human motion capturing system for home rehabilitation," Int Conf Mobile Data Management: Systems, Services and Middleware, pp. 359–360, 2009.

[47] V. Bonnet, C. Mazzà , P. Fraisse, A. Cappozzo, "A least-squares identification algorithm for estimating squat exercise mechanics using a single inertial measurement unit," J. Biomech., vol. 45, no. 8, pp. 1472–1477, 2012.

[48] V. Bonnet, C. Mazzà , P. Fraisse, A. Cappozzo, "Real-time estimate of body kinematics during a planar squat task using a single inertial measurement unit," IEEE Trans. Biomed. Eng., vol. 60, no. 7, pp. 1920–1926, 2013.

[49] V. Bonnet, V. Joukov, D. Kulic, P. Fraisse, N. Ramdani, G. Venture, "Monitoring of hip and knee joint angles using a single inertial measurement unit during lower limb rehabilitation," IEEE Sensors Journal, vol. 16, no. 6, pp.1557-1564, 2016.

[50] O. Giggins, D. Kelly, B. Caulfield, "Evaluating rehabilitation exercise performance using a single inertial measurement unit," Int Conf Pervasive Computing Technologies for Healthcare, 2013.

[51] J. Brutovsky, D. Novak, "Low-cost motivated rehabilitation system for post-operation exercises," IEEE Int Conf Eng Med Biol Soc, pp. 6663–6666, 2006.

[52] D. Fitzgerald, J. Foody, D. Kelly, T. Ward, C. Markham, J. McDonald, B. Caulfield, "Development of a wearable motion capture suit and virtual reality biofeedback system for the instruction and analysis of sports rehabilitation exercises," Int Conf IEEE Eng Med Biol Soc, pp. 4870-4874, Aug. 2007.

[53] S. Ananthanarayan, M. Sheh, A. Chien, H. Profita, K. Siek, "PT Viz: towards a wearable device for visualizing knee rehabilitation exercises," SIGCHI Conf Human factors Computing Systems, pp. 1247-1250, 2013.

[54] G. Lullini, L. Berti, M. Ortolani, A. Leardini, A. Valsecchi, "Are modern inertial sensor and bio-feedback based rehabilitation systems reliable enough? A validation study by standard gait analysis," Gait & Posture, vol. 39, supp. 1, pp. S42-S43, 2014.

[55] A. Leardini, G. Lullini, S. Giannini, L. Berti, M. Ortolani, P. Caravaggi, "Validation of the angular measurements of a new inertial-measurement-unit based rehabilitation system: comparison with state-of-the-art gait analysis," J NeuroEngineering Rehab, vol. 11, pp. 136, 2014.

[56] J.F.S. Lin, D. Kulic, "Human pose recovery for rehabilitation using ambulatory sensors," IEEE Int Conf Eng Med Biol Soc, pp. 4799-4802, 2013.

[57] M. Field, D. Stirling, M. Ros, Z. Pan, F. Naghdy, "Inertial sensing for human motor control symmetry in injury rehabilitation," IEEE/ASME Int Conf Advanced Intelligent Mechatronics, pp. 1470-1475, 2013.

[58] R. Houmanfar, M. Karg, D. Kulic, "Movement analysis of rehabilitation exercises: distance metrics for measuring patient progress," IEEE Systems Journal, vol. 10, no. 3, pp. 1014-1025, 2016.

[59] https://www.tyndall.ie/wireless-sensor-networks-2 (accessed 27/02/2017)

[60] R.M. Nilssen, J.L. Helbostad, "Estimation of gait cycle characteristics by trunk accelerometry," J Biomechanics, vol. 37, no. 1, pp. 121-126, 2004.

[61] M. Zhang, B. Lange, C.Y. Chang, A.A. Sawchuk, A.A. Rizzo, "Beyond the standard clinical rating scales: fine-grained assessment of post-stroke motor functionality using wearable inertial sensors," IEEE Eng Med Biol Soc, pp. 6111-6115, 2012.

[62] C. Strohrmann, R. Labruyere, C.N. Gerber, H.J. van Hedel, B. Arnrich, G. Troster, "Monitoring motor capacity changes of children during rehabilitation using body-worn sensors," J NeuroEngineering Rehab, vol. 10, pp. 83, 2013.

[63] N. Hogan, D. Sternad, "Sensitivity of smoothness measures to movement duration, amplitude, and arrests," J Mot Behav, vol. 41, no. 6, pp. 529-534, 2009.

[64] L. Schwickert, R. Boos, J. Klenk, A. Bourke, C. Becker, W. Zijlstra, "Inertial sensor based analysis of lie-to-stand transfers in younger and older adults," Sensors, vol. 16, no. 8, pp. 1277, 2016.

[65] S. Jiang, B. Zhang, D. Wei, "The elderly fall risk assessment and prediction based on gait analysis," IEEE International Conference on Computer and Information Technology, pp. 176-180, 2011.

[66] M. Gietzelt, G. Nemitz, K.H. Wolf, H.M.Z. Schwabedissen, R. Haux, M. Marschollek, "A clinical study to assess fall risk using single waist accelerometer," Journal Informatics for Health and Social Care, vol. 34, no. 4, 2009.

[67] https://uk.mathworks.com/products/matlab.html (accessed 27/02/2017)

[68] T. Seel, J. Raisch, T. Schauer, "IMU-based joint angle measurement for gait analysis," Sensors, vol. 14, no. 4, pp. 6891-6909, 2014.

2017, © Copyright by authors, Published under agreement with IARIA - www.iaria.org